DEVELOPMENT OF SPACE-INVARIANT SIGNATURE ALGORITHM (*SISA*) - AN INNOVATIVE APPROACH FOR PROCESSING THE MEDICAL IMAGES FOR THE DETECTION AND LOCALIZATION OF EARLY ABNORMALITIES IN BIOLOGICAL TISSUES

A Thesis Submitted to the College of Graduate Studies and Research

In the Partial Fulfilment for the Requirements

Of the Degree of Master of Science

In the Division of Biomedical Engineering

University of Saskatchewan

Saskatoon, Canada

By

Kushagra Parolia

June 2016

PERMISSION TO USE

In presenting this thesis in partial fulfilment of the requirements for Master of Science degree from the University of Saskatchewan, I agree that the Libraries of this University may make it freely available for inspection. I further agree that permission for copying of this thesis in any manner, in whole or in part, for scholarly purposes may be granted by the professor or professors who supervised my thesis work or, in their absence, by the Chair of the Division or the Dean of the College in which my thesis work was done. It is understood that any copying or publication or use of this thesis or parts thereof for financial gain shall not be allowed without my written permission. It is also understood that due recognition shall be given to be and to the University of Saskatchewan in any scholarly use which may be made of any material in my thesis. Requests for permission to copy or to make other use of material in this thesis in whole or part should be addressed to:

Head of the Division of Biomedical Engineering

57 Campus Drive

College of Engineering

University of Saskatchewan

Saskatoon, SK

Canada S7N 5A9

ABSTRACT

Early detection, diagnosis and localization are some of the important issues facing the medical profession for diseases such as cancer and cardiac disorders. Therefore, it is vital that a reliable approach, which is economic, safer and less time consuming be developed for the detection and diagnosis of such disorders. In this thesis an innovative approach, **S**pace-**I**nvariant **S**ignature **A**lgorithm ***(SISA***) is proposed and developed to process the medical images for the detection and localization of abnormalities at an early stage in active biological tissues such as cancer, potential tumor growth and damaged tissues. In this proposed *SISA* approach, if the *SISA* signature pattern is *space-invariant* it suggests the absence of any abnormality. A *space-variant SISA* signature pattern is an indication of the presence of the abnormality. The abnormality in an active system can be defined as the obstacle, which impedes the smooth flow of activities such as blood or electrical signals. In any active system under excitation, abnormalities create extra perturbations, depending on the stage of progression of the abnormality. An abnormality in the final stage or critical stage will create very high perturbations that would largely impede the smooth flow of the excitation, whereas, in early stages, the abnormality will create low perturbations and would slightly impede the smooth flow of the excitation provided to the active system. Using the *SISA* approach, in the absence of any abnormalities, the signature pattern should have a uniform signature pattern, whereas, in the presences of abnormalities, the *SISA* signature pattern will be

space-variant. The degree and position of the variance in space helps in the detection and localization of the abnormality.

The *SISA* approach was first tested on a liquid vibrating system with various types of obstacles. These abnormalities created perturbations in the system parameters that induced the vibration patterns. Furthermore, the experimental results using the *SISA* approach were also obtained on ultrasound images to find abnormalities in animal tissues. In each of these cases of ultrasound imaging, the *SISA* signature patterns were able to localize and detect the tissue abnormality.

The experimental results obtained with various types of small and large impedances (obstacles), which represent respectively the early and critical stages of abnormalities in the vibrating liquid system, were very encouraging. This basic *SISA* study on the liquid vibrating system was extended for processing ultrasound images for the detection and localization of damaged biological tissues. These initial experiments on animal tissues using ultrasound images along with *SISA* processing indicate that this innovative *SISA* approach has a great potential for processing other types of medical images such as ultrasound, Magnetic Resonance Elastography (MRE) and Computed Tomography (CT scan) for the detection and localization of abnormalities at an incipient stage.

ACKNOWLEDGMENTS

I am very happy to acknowledge and express sincere gratitude to my co-supervisors, Professor Madan M. Gupta, Dr. Paul Babyn and Professor Wenjun (Chris) Zhang who gave me constant encouragement, invaluable patience and tremendous support during this research work. Their wisdom and insight were a beacon of hope, greatly improving the work slowly and steadily every day.

I also express my wholehearted thanks to the members of the advisory committee: Dr. Dean Chapman and Professor Aryan Saadat Mehr; their suggestions and ideas have greatly improved the present work.

I would like to thank Douglas Bitner for his direction and kind offering of laboratory equipment for performing experiments and Tung Nguyen, for helping in the development of the *SISA* program. The help from the support staff of the Medical Imaging group at the Royal University Hospital is greatly appreciated.

My research was made possible by the generous support of Division of Biomedical Engineering, University of Saskatchewan through graduate scholarship and Graduate Students' Association through their bursary program.

DEDICATION

To my parents Manisha and Praveen Parolia for always encouraging me to pursue knowledge and benevolence. To my sister Mimansa, who is a constant inspiration with her lovely smile.

To my best friend Natalia Cavalca Cardoso, for being with me during this research.

TABLE OF CONTENTS

LIST OF FIGURES

LIST OF ABBREVIATIONS

AKI	Acute kidney injury
ECG	Electrocardiogram
FNAB	Fine-Needle Aspiration Biopsy
MRE	Magnetic Resonance Elastography
MRI	Magnetic Resonance Imaging
PISA	Phase-Invariant Signature Algorithm
ROI	Region of interest
SISA	Space-Invariant Signature Algorithm
TISA	Theta-Invariant Signature Algorithm
US	Ultrasound

Chapter 1

INTRODUCTION

1.1 Space-Invariant Signature Algorithm *(SISA):* Some Motivations

Space-Invariant Signature Algorithm (*SISA*) is an innovative approach developed in this thesis, for processing the medical images such as ultrasound (US) and magnetic resonance elastography (MRE), used in the detection and localization of abnormalities at an early stage in biological tissues.

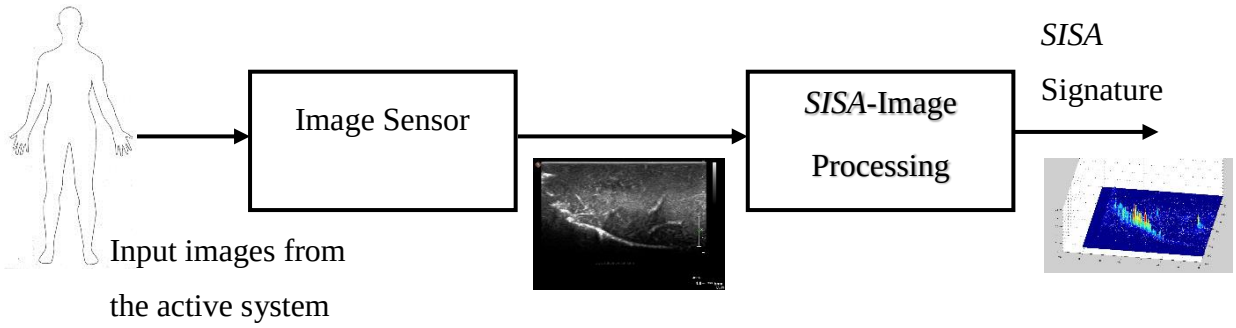

Figure 1.1: Block diagram for the SISA approach

SISA approach requires an image sensor, and these images are processed using the *SISA* algorithm to obtain *SISA* signature pattern. The image sensor such as a digital camera or an ultrasound probe that can be used to capture the digital images and ultra-sonographic images respectively, are shown in Figure 1.1. These images are captured non-invasively from an active system, i.e. human body, and *SISA* signature pattern provides information about the presence of abnormalities in the active system. The *SISA* processing approach is inspired and extended from the Phase-Invariant Signature Algorithm (*PISA)* technique, which was developed for testing the

animals and humans for the detection and diagnosis of ischemic heart diseases [2]. In the following section we briefly describe the *PISA* technique.

1.2 Phase-Invariant Signature Algorithm *(PISA)* Approach for the Detection and Diagnosis of Ischemic Heart Disease

PISA is an extension of the Theta-Invariant Signature Algorithm (*TISA*). *TISA* was developed for the detection and diagnosis of incipient failures in rotating machines [1]. To determine the incipient failure in rotating machines, an angle was assigned over 0^o to 360^o rotation, and the measurements of vibrations were taken at a fixed angle (Θ). The measured vibration signals from rotating machines were then processed to obtain the *TISA* signature pattern, which helps us in determining the presence of an abnormality [1].

PISA was used for detection of ischemic heart diseases, using high-frequency electro-cardiac signals [2]. In the cardiac system, cardiac electric impulses are generated by heart at the Sino atrial node (SA node). These electric impulses spread around the cardiac system passing through various active cardiac tissues [1, 2]. An electrocardiogram (ECG) is a measurement of the electrical activities of the cardiac system, which is periodic repeating from 0 to T seconds as a function of time or homogeneously, as a function of phase 0 to 2π radians. A conventional ECG has low-frequency measurements and has been used extensively for the detection of cardiac abnormalities, which filters out the higher frequencies using a low pass filter. Since the measurements in the ECG are mainly at the low-frequency detection range, the high-frequency information generated by early heart problems go unobserved, leading ECG to a reduced

sensitivity for detecting ischemic heart diseases [2]. Usually, in ECG by observing the T-inversion and/or variation in the S-T segment, the abnormal cardiac tissues can be determined.

In the *PISA* approach, the processing of electro-cardiac signals is done with a bandwidth of about 10 kHz, as compared to 50-100Hz of conventional ECG. Cardiac electrical activities generated in the heart by SA node pass through ischemic dead cells. The ischemic dead cells to an extent impede the flow of electrical activities generating high-frequency perturbations in electro-cardiac signals [2]. The *PISA* approach is able to detect these high frequency perturbations caused by the abnormal cells and detect the ischemic heart disease at an early stage [2]. The *PISA* approach has also been used for the detection and diagnosis of heart problems, for example detecting valve leakage in the heart [2]. More information on the *PISA* approach is discussed in Appendix B.

1.3 Importance of Non-Invasive Techniques in the Early Detection of Abnormalities

In this section, the importance of early detection is discussed and how the *SISA* processing with its full potential can help make a difference in detecting abnormalities with the help of other non-invasive medical imaging techniques.

Human body comprises of small individual active systems such as circulatory system, muscular system etc. working tirelessly every day, every moment. Our bodies are very dynamic in nature with so many hidden characteristics happening at that same time. On a cellular scale, new cells are created every second and old ones are replaced.

Why do early detection? Why early detection for cancer or any abnormality? In order to answer these questions, it is necessary to answer them separately. Cancer is not just one disease it is a collective term for abnormal activities, which go through a similar multistep development of tumors in human beings [3, 4]. Cancer may seem to be looking similar from the outside but each type of cancer develops differently in different way and can originate in any type of tissue. To understand the cancer in a brief definition, it begins during the formation of new cells which are created to form tissues and organs such as muscles or bones, a mutation in cell reproduction may also create some abnormal cells, but our bodies are highly efficient in identifying these mutations removing the cancerous or abnormal activities by themselves.

But some cells with specific mutations are able to evade the immune system and become benign (non-cancerous) or malignant (cancerous) tumors. Benign tumor cells are usually dormant and is not generally life threatening. Whereas malignant cells are more active, life threatening and can also cause metastases [5].

Generally, for the complex life form such as humans or animals, as the time or age progresses in any the problem or disorders progresses with it. People tend to be healthy when young and slowly their health deteriorates with age, similarly with animals. During the regular check-ups, if the problem is detected at early stage, it reduces the treatment time, money and risk of life. However, the later the disease is detected, the lower the chance of complete recovery and higher the treatment time is required with money and additional resources perhaps needed to fight the problem. At early stages of the disease, it is easier to handle and very economically to treat the disease as compared to later or critical stages. The challenge with early detection is that, it is very hard to detect the problem.

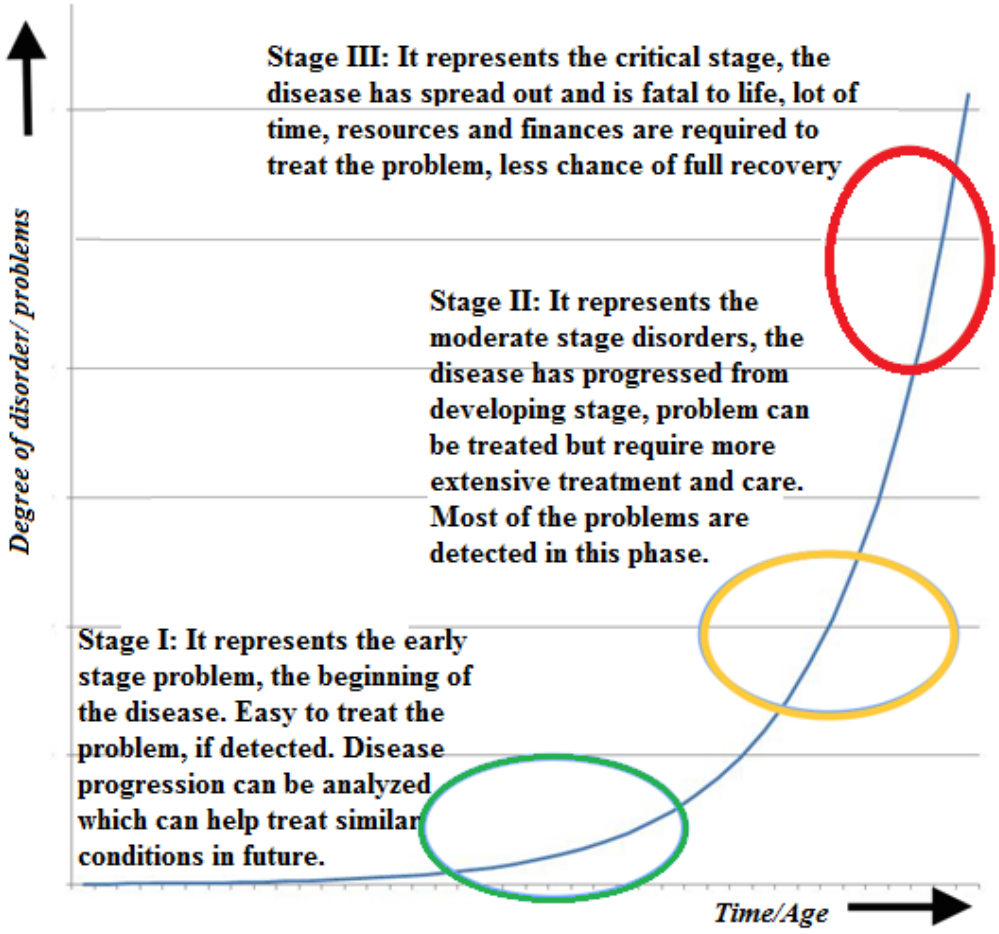

Figure 1.2: Progression of diseases over time, problems/disorder vs time/age

When the disease has progressed to the moderate stage or stage II (Figure 1.2) by the time the disease is detected, diagnosed and the treatment is started, it is either already too late to understand the foundation of the disease and the recovery time is much higher than that in stage I, and with a relatively higher cost of expense.

Stage III is the last or the critical stage, it is a life-threatening stage, requires a lot of human and technological resources, with chances of recovery being low. It is important to note that in Figure 1.2, x-axis has time/age as variable, because the disease sometimes can affect the

individual regardless of age, and progresses with time. Various factors affect the progression of time, due to which it might take longer to reach the stage II and III.

According to the survey, in 2015, from Canadian Cancer Society it is expected that 2 in 5 Canadians will develop cancer in their lifetimes. Males have a 45% lifetime probability (or a 1 in 2.2 chance) of developing cancer [6]. Several factors work together increasing the likelihood survival for the patients. These factors include the stage of cancer at diagnosis and aggressiveness of the tumor, as well as the availability and quality of early detection and treatment services, with other factors such as age, sex, health condition and general lifestyle [6, 7]. It is necessary to use a non-invasive technique for early detection of abnormalities in active systems, for further analysis and diagnosis of progression of the disease.

Canadian Cancer Society lists early warning signs of cancer, which extends from unusual lumps to unexplained aches and pains [10]. In most of the cases of breast cancer and ovarian cancer, the use of ultrasound is predominated for early check-ups and the doctor forwarding for further analysis. This makes it really challenging to cover a large portion of warning signs, and to examine the data from the patients, with a possibility of cancer. Cancer Cell Line Encyclopaedia lists 36 tumor types, which is an ongoing project with more data to be studied, to enable predictive modeling of anticancer drug sensitivity [11]. These different types of abnormalities are hard to detect in the first glance in their early stages and being forwarded for a quick diagnosis by a doctor.

Non-invasive medical imaging has proven to be better choice in terms of early detection. In recent studies [6, 7, 12] the decrease in cancer deaths in females is attributed to declines in breast

cancer mortality, which is further likely due to improvements in early detection and screening as well as advances in treatment and related improvements in treatment outcomes. Not only in breast cancer but ranging from unusual lumps to pelvic masses, non-invasive imaging such as ultrasound is highly recommended before further diagnostics [6, 7, 12]. There is a need to develop an algorithm to check these abnormal behaviours and detect their development and provide a diagnosis, which can help not only doctors or patients but also use of resources and technology.

Etzioni et al in their study has mentioned the advantages and disadvantages of non-invasive and discuss the essential properties of a detection technique [9]. For early detection to be an effective approach, the early abnormality testing should meet following criteria such as [2, 9]:

1) Early detection test should demonstrate a high degree of accuracy, able to distinguish between healthy and unhealthy individuals with a specific threshold value,

2) It should be able to detect before progressing towards advanced stage making it less use for the test,

3) The screening tests should provide a difference between aggressive lesion and non-aggressive lesion avoiding over-diagnosis,

4) Early detection should be inexpensive and well accepted by target population,

5) The test should be easily reproducible.

Although other techniques such as early detection using biomarkers are promising, but biomarker development requires detection of both clinical and pre-clinical disease, and dissemination of screening tests that have been inadequately evaluated can have grave

consequences, including increased medical costs, unnecessary treatments and invasive follow-up of healthy individuals [13].

With some advantages to non-invasive early detection, there are some disadvantages too. Due to the complex structure of the human body as an active system, it is very hard to generalize the results for one specific person. This dynamic nature not only gives a challenge to early detection but also to create boundaries for us. As the disease progresses from the early stages, it is possible to detect the disease through regular check-ups with a doctor and using currently established medical imaging techniques such as ultrasound, MRE, and CT-scan. These medical imaging techniques require expert eyes in order to detect and further analyze the cause of the disease in its early stages, with a developed algorithm it is possible to detect large amounts of data for a large number of patients, and determine the abnormality in its incipient stage.

From this discussion it can be concluded that early detection is a very important aspect for a healthy lifestyle, and non-invasive techniques offer a painless, safe and promising results in detecting major diseases.

1.4 Research Objectives

Objective 1:

To develop a medical image-processing algorithm, Space-Invariant Signature Algorithm (*SISA*), which would help in the detection and localization of abnormalities at an early stage.

The scope of research with this objective is: (1) to assess *SISA* image processing technique, (2) to determine its ability in the detection of the abnormalities in an active system, (3) to understand the limitations and applicability of *SISA* in the active system, and (4) to improve it further.

Objective 2:

To use medical imaging techniques such as ultrasound for further expansions of *SISA* towards biological tissues using pig and chicken tissue sample models, and to determine its ability to detect the abnormalities.

The scope of research with this objective is: (1) to further enhance the *SISA* signature pattern by conducting more experiments on the animal tissue model and (2) to determine the threshold values for specific types of animal tissue models and to detect and localize the abnormality with other medical imaging techniques.

Chapter 2

DEVELOPMENT OF SPACE-INVARIANT SIGNATURE ALGORITHM (*SISA*)

2.1 Space-Invariant Signature Algorithm (*SISA*)

In this chapter, the assumptions and mathematical formulation to achieve the *SISA* technique are discussed in detail.

SISA approach developed in this research work concerns the early detection and localization of abnormalities in active systems using images. To understand the common terminology used in this thesis, it is necessary to understand concepts such as what does an activity and abnormality mean. In this research, an activity can be defined as the degree to which something displays its characteristics property or behavior. An abnormal activity, which is generally created by abnormalities present in the active system, displays anomalous behavior in terms of random perturbations. Abnormality (in brief) can be described as something, which is changing or has been changed from the normal functional activity, creating undesirable consequences in the active system. These abnormalities induce non-linear impedances, which restricts the smooth flow of activities such as blood, vibrations or water flow. Abnormalities can be cancer cells, damaged tissues, dead cell accumulation and tumor growth. An active system is dynamic in nature and evolves with time. For example, human body is an active system and abnormalities in human body such as external and internal injuries and benign and malignant tumors induce perturbations in the dynamics of the system. Using advancement in medicine and technology,

these abnormalities in human body could be detected and treated at the moderate stage, when signs and symptoms appears. *SISA* approach is developed for the detection and localization of abnormalities in early stages.

2.2 General Concepts of *SISA*

In this thesis, *SISA* approach is presented and tested on a liquid vibrating system and several biological tissues, which is explained in detail in the next chapter. In *SISA* analysis, a measured image of an active system is assumed as consisting of three main components: i) the external carrier signal (excitation) which is pre-set and supplied to the system and is deterministic (stationary) in nature, ii) the information generated by abnormal activity, which is random in nature and signifies the presence of an abnormality, iii) the background measurement noise generated from various surrounding sources. In a normal active system, the random information generated by abnormal activities will be absent. The 3D graphic representation of the characteristic behavior of an active system processed through *SISA* approach is called as *SISA* signature. When an abnormal behavior is present, it tends to produce a change in its surrounding by restricting the normal flow in the system and creating random perturbations, which are absent in normal active system. The *SISA* signature pattern shows these random perturbations, for example in the presence of the abnormality, the *SISA* signature pattern observed is irregular, uneven or space-variant. In the absence of the abnormality, the *SISA* signature pattern observed is uniform, flat or space-invariant. Therefore, *SISA* signature displays the presence or absence of the abnormal activity. The space-invariant pattern achieved from a normal active system acquires the name “Space-Invariant Signature Algorithm (*SISA*)”.

The external carrier signal (excitation) is a stationary component and is uniformly distributed all over the active system, whereas random perturbations caused by the information are hard to detect, as their location and existence is previously not determined. These measured image components are present in the image in form of pixels. Any digital image is made of pixels or dots per inches (dpi). Different parts of the image are variations in pixel intensity. To understand the reason behind this it is necessary to know that there are mainly two types of images: incoherent and coherent images. The incoherent images are taken under specific lightening or natural light and coherent images are obtained from holograms, ultrasound images or radar. The pixel to form an image (coherent or incoherent) is made from the combination of the energy from all the sources. In this research, both incoherent (camera image) and coherent (ultrasound image) type of images are used to process the signature pattern. For the liquid vibrating system, a digital camera was used and for experimentation on tissues, an ultrasound machine was used.

The *SISA* pattern in the region of interest contains the signature for the abnormal behavior of the system, which will be space-variant. To test our hypothesis, an experiment was performed to analyze the behavior of the abnormality in a *simulation* of an active system such as liquid container with pseudo-random wave excitations as external carrier. The proposal behind this approach is that, when the active system under an external carrier or excitation is introduced with an abnormality, it creates extra perturbations that are detected and localized in the *SISA* signature pattern. The magnitude of the perturbations is detected on *SISA* signature pattern depending on the present stage of the abnormality such as early stage (Stage I) or critical stage (Stage III). For example, if the abnormality is in critical stage, it will create high frequency perturbations, on the other hand, if the abnormality is in early stages, it will create low frequency perturbations that provide an idea of possible present stage of the abnormality.

As the abnormality progresses from early to advanced stage, the low power magnitude created by the perturbations increases, implying the advancement of the disease. For a normal active system, the *SISA* processing yields a signature pattern, which is a space-invariant signature whereas in the presence of abnormalities an extra information component will exist. Basically, a signature pattern using the *SISA* approach is the detection of extra perturbations created by the abnormality, which can be distinguished clearly as compared with the normal behavior of the system.

It is to be noted that the term obstacle is used in order to represent an abnormality in a liquid vibrating experiment, the objects such as perforated obstacle and solid obstacle. The perturbation waves and ripples created by them obstruct the flow of pseudo-random waves normally in the same container. In case of ultrasound analysis (in Chapter 4) the term abnormality is used, as in a biological system, or in medical terms it is more appropriate to address obstruction or impedance, as a defect or an abnormality.

2.2.1 Comparison between the *PISA* and *SISA* techniques

The *PISA* and *SISA* techniques are very similar to each other and they share a common element that is the final signature being invariant signifying that in the absence of an abnormality the final processed graph will result in uniform or invariant output. Whereas, in the presence of an abnormality the signature pattern will be non-uniform or variant, indicating the presence of an abnormal activity.

Regardless of their similarities, *PISA* and *SISA* also possess some major differences, which can be understood from the following two main points: Firstly, in *PISA* it is assumed that ECG signal from abnormal heart is composed of three main components: (i) the electrical activity

from normal cardiac cells, which is deterministic periodic process; (ii) the electrical activity from abnormal cardiac cells, which is random in nature, phase-locked to heart cycle; (iii) the background noise measurement generated from different sources [2]. Whereas in *SISA*, it is assumed that the measured signal in the form of images is composed of three main components: (i) the external carrier provided to the system, which is a deterministic representation of the image; (ii) the information, which is the key to defining the abnormal activity and random in nature and is confined to region of interest by image sensor; (iii) the noise generated from surroundings and image signal. Second, in *PISA*, random perturbations in the electrical activity of the heart measured from ECG are phase-locked [2]. Whereas in *SISA*, the random perturbations measured in the active system are restricted to the measured region of interest or space-locked. Finally, *PISA* method was developed to process the electro-cardio and phono-cardio signals, whereas *SISA* method is developed to process the digital images.

2.2.2 Mathematical Formulation of *SISA* approach

In this section, the mathematical formulation of the *SISA* approach for the detection of early abnormalities in active system is described in detail. As mentioned previously, in developing the *SISA* approach it is considered that the measured image (M_k (i, j)) has the following three components:

C_k *(i, j): the carrier that represents the image of the deterministic (stationary) activities in the system.*

I_k *(i, j): the random information generated by the abnormal activity. The abnormality in the active system creates random perturbations and provides non-linear impedance building an obstruction in smooth flow activities such as liquid or blood; detection of these random perturbations is an indication of the presence of abnormalities in active system.*

$N_k(i, j)$: the random activities caused by noises in the active system, which are equally distributed throughout the system.

(i, j): represents x-axis and y-axis of a matrix space in the image, which is kept fixed at the region of interest, while taking the measurements, and the z-axis represents the SISA scale, particularly if it is space-invariant then no abnormality is present, and if the z-axis is space-variant then the abnormality is present.

k: represents the number of images

In the mathematical formulation, the signature pattern is represented by (Sig (i, j) or $\bar{V}(i,j)$), during the measurements the signal received contains three main components as mentioned above, all of which are collectively called the measured image, denoted as "M_k *(i, j)*", which is processed further with the detailed algorithm discussed below to obtain the signature pattern (Sig (i, j) or $\bar{V}(i,j)$).

For obtaining the *SISA* signature pattern, statistical processing was done using 'n' number of images, which ranges from 100-200 images depending on the experiment. In the liquid vibrating system experiment, about 100 images were used for different type of abnormalities and in the ultrasound analysis, about 200 measured images were captured for the *SISA* processing.

In our formulation it is assumed that each measured image is given by:

$$M_k(i,j) = [C_k(i,j) + N_k(i,j) + I_k(i,j)] \quad \ldots\ldots\ldots\ldots\ldots\ldots \quad (2.1)$$

where, k= 1, 2,...n, and the measured image "M_k" is a function of space coordinates (i, j). By taking the ensemble average of the images, Equation (2.1) becomes:

$$\mu(i,j) = \bar{M}(i,j) = \frac{1}{n}\sum_{k=1}^{n}\left(M_k\,(i,j)\right)$$

$$= \frac{1}{n}\left[\sum_{k=1}^{n} C_k\,(i,j) + \sum_{k=1}^{n} N_k(i,j) + \sum_{k=1}^{n} I_k(i,j)\right] \ldots\ldots\ldots \quad (2.2)$$

where, $k = 1, 2 \ldots n$. Rewriting Equation (2.2) as follows:

$$\mu(i,j) = \bar{C}(i,j) + \bar{N}(i,j) + \bar{I}(i,j) \ldots\ldots\ldots\ldots\ldots \quad (2.3)$$

From Equation (2.3), $\mu\ (i, j)$ is the ensemble average of all the $M_k\ (i, j)$. The carrier C_k represents the deterministic portion of the image, hence, the ensemble average of all carrier components will be $\mu\ (i, j) = \bar{C}$, as C_k is constant during the whole experiment.

The ensemble averages of random activities; I_k and N_k will be zero.

Therefore $\bar{I}(i,j) = 0$, and $\bar{N}(i,j) = 0$

As C_k is a signal, it is kept constant throughout the measurement. Using Equation (2.3) the ensemble average of measured images, $\mu\ (i, j)$ is given by:

$$\mu(i,j) = \frac{1}{n}\sum_{k=1}^{n} C_k\,(i,j) \ldots\ldots\ldots\ldots\ldots\ldots\ldots \quad (2.4)$$

To calculate the variance, Equation (2.1) and (2.2) were used.

The *SISA* signature, before taking the ensemble average, is defined as follows:

$$V_k(i,j) = [M_k(i,j) - \mu(i,j)]^2$$

$$V_k(i,j) = \left[M_k(i,j) - \frac{1}{n}\sum_{k=1}^{n} C_k\,(i,j)\right]^2 \ldots\ldots\ldots \quad (2.5)$$

Therefore, the *SISA* signature pattern, (Sig (i, j)) is defined as:

$$Sig\ (i,j) = \bar{V}(i,j) = \frac{1}{n}\sum_{k=1}^{n} V_k(i,j)$$

$$= \frac{1}{n}\sum_{k=1}^{n}[N_k^2(i,j) + I_k^2(i,j) + 2.N_k(i,j) \times I_k(i,j)] \ldots\ldots \quad (2.6)$$

Since the random activities, N_k and I_k, arise from independent and unsystematic events, they are uncorrelated, and two jointly normally distributed random variables are independent if they are uncorrelated. If two variables are uncorrelated, there is no linear relationship between them.

In Equation (2.6), the product of two uncorrelated variables (noise, N_k and information, I_k component) is zero, as previously mentioned that they are independent random variables, therefore it can be concluded that their product will be zero.

$$N_k(i,j) \times I_k(i,j) = 0 \quad \ldots\ldots\ldots\ldots\ldots\ldots\ldots\ldots\ldots\ldots \quad (2.7)$$

Therefore, Equation (2.6), to obtain *SISA* signature, can be rewritten as:

$$Sig(i,j) = \frac{1}{n}\sum_{k=1}^{n}[\, N_k^2(i,j) + I_k^2(i,j)] \quad \ldots\ldots\ldots\ldots\ldots\ldots\ldots\ldots\ldots\ldots \quad (2.8)$$

From Equation (2.8), it should be noted that the *SISA* signature pattern consists of the following three parts:

(i) Ensemble average of square of the information component that exists due to the random activities generated by the abnormality in the active system. In the final Equation (2.8) 'I_k' is squared and ensemble averaged over 'n' number of images. In the SISA signature pattern, variable 'I_k' plays an important role in determining the stage of the problem.

(ii) Ensemble average of square of the noise component, which occurs due to the random activities in the active system, and is uniformly distributed throughout the invariant space. In the final Equation (2.8) the square of 'N_k' and the ensemble average over 'n' number of images is present, when it is ensemble averaged over 'n' it overall adds up uniformly all over the SISA signature pattern.

(iii) Sig (i, j), or $\bar{V}(i,j)$, is the final result image after processing all the images, which detect the position of abnormality, the higher the number of images 'n', the better the 'Sig (i, j)' is achieved. The optimized number of images of about 100 to 200, based on the experience is used for SISA processing.

The block diagram in Figure 2.2 illustrates the steps, from the mathematical formulation, for obtaining the *SISA* signature pattern. The signal incoming from the sensor comprising of carrier signal, representing the deterministic part of the system, noise signal, and information component measured regarding the presence of abnormality in the system. The signal in form of images is ensemble averaged, denoted as ($\bar{M}(i,j) or\ \mu(i,j)$), then $\bar{M}(i,j)$ is subtracted with the measured image (M_k), and the ensemble average of the square of $[M_k(i,j) - \bar{M}(i,j)]$ to obtain the variance, namely the *SISA* signature pattern (Sig (i, j), or $\bar{V}(i,j)$).

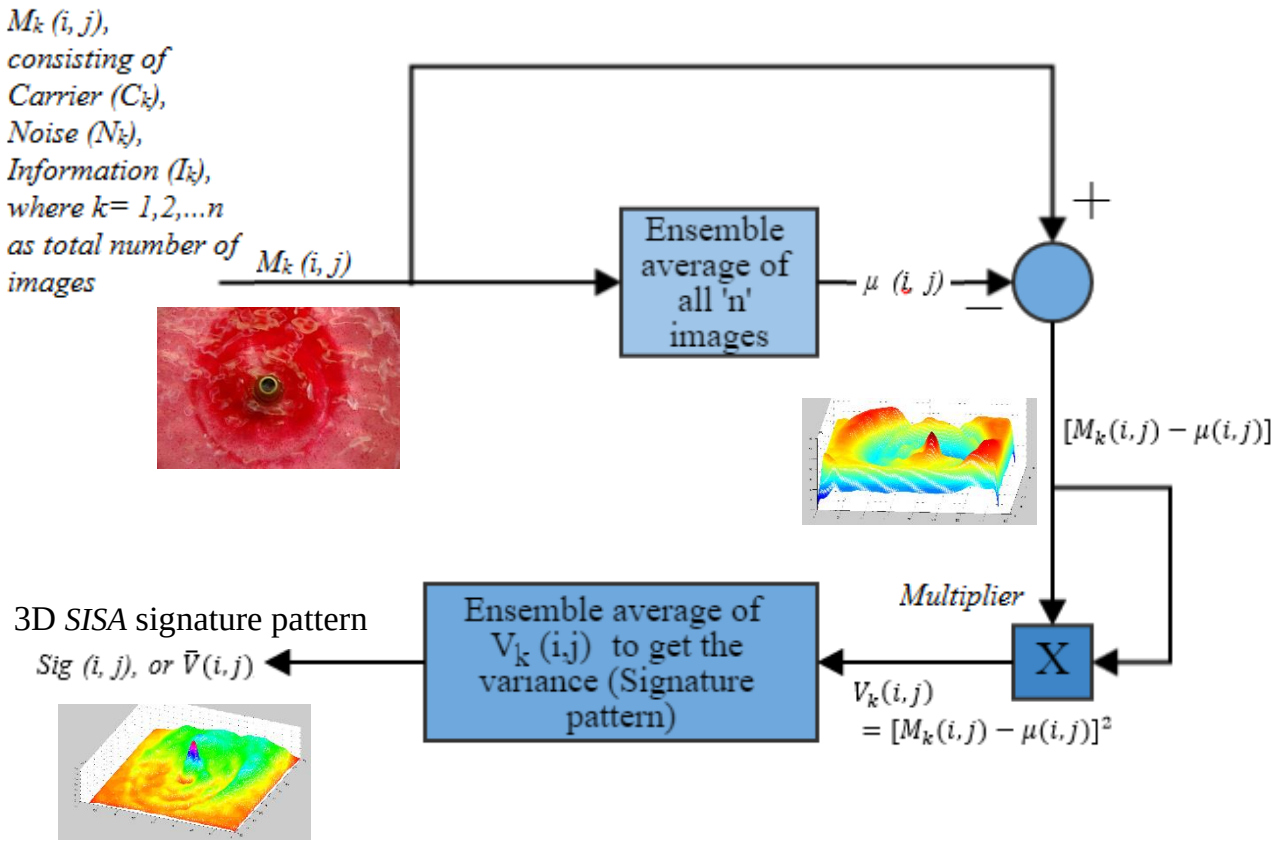

Figure 2.2: Flowchart with mathematical formulation for the SISA processing, I_k represents the Information, which indicates the presence of abnormality.

Chapter 3

EXPERIMENTS FOR DETECTION OF ABNORMALITIES IN LIQUID VIBRATING SYSTEMS: SOME PRELIMINARY UNDERSTANDING

3.1 Introduction

This chapter contains a comprehensive description of the experiment with liquid vibrating systems. The purpose of this experiment is to provide a preliminary understanding of the feasibility of the *SISA* approach. This active vibrating system was considered as a very simple model to an active system. The general idea of the experiment is that if an abnormality is present some random perturbations would be created in the system while the excitation is provided and the *SISA* method would detect the perturbations caused by the abnormality and thus the abnormality. After experimenting with different trial and error methods the following results were obtained. Different types of obstacles were put in a liquid system of finite and infinite impedance. The finite impedance of the obstacle closely relates with a partial hindering and generating some low perturbations, while infinite impedance of the obstacle is analogous to a complete hindrance creating high perturbations, with the analogy to early and critical stage of the abnormality respectively, in the active system. The information about the obstacles such as their location and shape is known in Priori. Excitation with the bandwidth of 100 Hz was produced in the liquid in the system to create vibration or wave of the liquid. The behaviors of the wave for the system without any obstacle and for the system with the obstacles were measured. The behaviors were then analyzed with the *SISA* procedure, aiming to conclude where and what

obstacle lies in the liquid system. It is noted that the wave is created in a random manner, and the excitation is thus called the pseudo-random excitation.

3.2 Experimental Setup for Liquid Vibrating Systems

Experimental setup for vibrational analysis consists of five main components: 1) Dual channel signal analyzer, 2) Multi-vibration exciter, 3) Oscilloscope, 4) Amplifier and 5) Digital camera. The pseudo-random wave was created in the dual channel analyzer, which was connected to the amplifier and oscilloscope. Oscilloscope from the source displayed the pseudo-random wave generated. Amplifier was connected to the multi-vibration exciter. Multi-vibration exciter created the pseudo-random vibrations in the liquid container. The detailed description of equipment is discussed as follows:

Dual channel signal analyzer

The dual channel signal analyzer used was made from vacuum tubes instead of transistors and provided a very precise pseudo-random signal, with adjustable bandwidth frequency. Pseudo-random signal, used from dual channel analyzer is made up of a segment of a "random" signal of a certain time period 'T' and is repeated after every period of time T. The bandwidth for the pseudo-random wave was selected as 100Hz after trial and error approach in order to achieve the best image with wave formations at the region of interest. Dual channel analyzer was used to provide the excitation, which varied from the pseudo-random to the pre-defined frequencies ranging from 50Hz to 100Hz. Dual channel signal analyzer, was used for the purpose of wave generation, which provided a pre-defined pseudo-random wave of 100Hz bandwidth for the experiment.

Oscilloscope

Agilent DSO6014A Oscilloscope was used for the examination of the generated wave as shown in Figure 3.1. The oscilloscope was connected with the dual channel analyzer and in parallel connection with the amplifier. The pseudo-random wave generates was displayed on oscilloscope screen with the frequency and amplitude. To keep conditions ideal for the different type of experiment for the liquid vibrating system it was necessary to monitor the wave generation.

Amplifier

The pseudo-random wave generated from dual channel analyzer was transferred to the amplifier to increase the power of the signal in order to observe the vibration pattern on the liquid container.

Multi-vibration exciter and digital camera

In Figure 3.1, the experimental setup with digital camera setup and the liquid container mounted on the Multi-vibration exciter is shown. Proper lighting to observe the wave patterns was used to take the measured images in best possible ways. Multiple shots were taken without flash, with the up to a total of 100 images for liquid vibrating system experiment. Multi-vibration exciter connected with the amplifier-generated vibrations from the pseudo-random waves.

In summary, a pseudo-random signal of bandwidth 100Hz was generated through the dual signal analyzer, which was connected with oscilloscope and amplifier, to display and amplify the signal generated, respectively. The amplifier was further connected with the multi-vibration exciter, which created vibrations. On top of the multi-vibration exciter, a circular container with

a liquid solution was mounted to observe the wave patterns generated in the liquid, due to pseudo-random vibrations. The choice of a circular container was made due to better positioning and wave generations. This experiment was conducted using a circular container with a liquid solution that consisted of water and jelly powder mixture to make the solution more viscous in nature and for better image capturing and analysis.

The camera was focused on the region of interest (ROI), of the container in order to achieve the best possible wave pattern generated by the exciter and to avoid the ripples created from the container walls. Lastly, the digital camera was fixed in space in order to capture space-invariant measurements to capture the wave patterns in the container and obtain measured image "M_k (i, j)" as explained in the previous section 2.2.1.

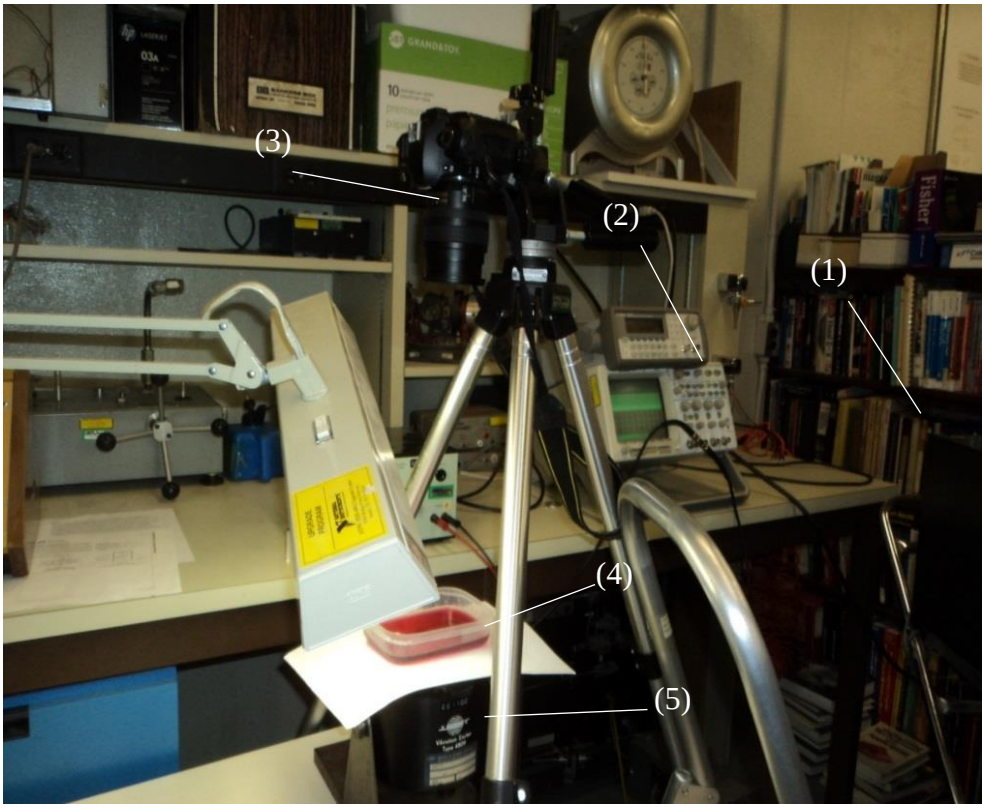

Figure 3.1: Experimental setup for liquid vibrating system, (1) Dual channel analyzer, (2) Oscilloscope, (3) Digital Camera, (4) Liquid container, (5) Multi-vibration exciter

3.3 Results of the *SISA* Analysis on the Liquid Vibrating System

3.3.1 Pseudo-Random Excitation without any Abnormality

The first experiment in a liquid vibrating system was conducted without any obstacle, signifying that- 'no abnormality/no obstacle' was present in the liquid container, representing a normal active system; with no extra frequency components are created due to the absence of abnormality. This way an analysis of *SISA* signature pattern was made for the normal state of the liquid vibrating system. And based on the observations, the subsequent deduction of the *SISA* signature pattern was made under similar conditions that it was found that in our experiments on the scale of 'z-axis', which in our work is called as the signature pattern., the magnitude of the signature pattern doesn't exceed more than 2×10^{-3} in the cases of 'no obstacle'.

(a) Raw camera image of a vibrating system without any abnormality

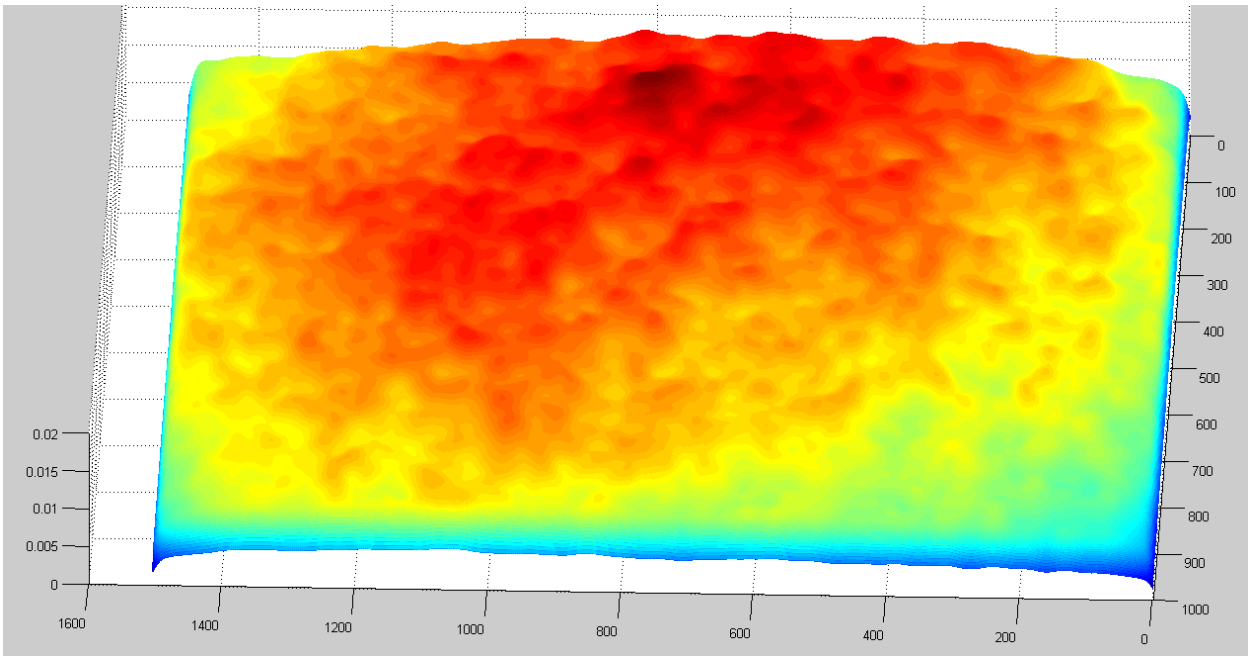

(b) Ensemble average of images in a normal vibrating system

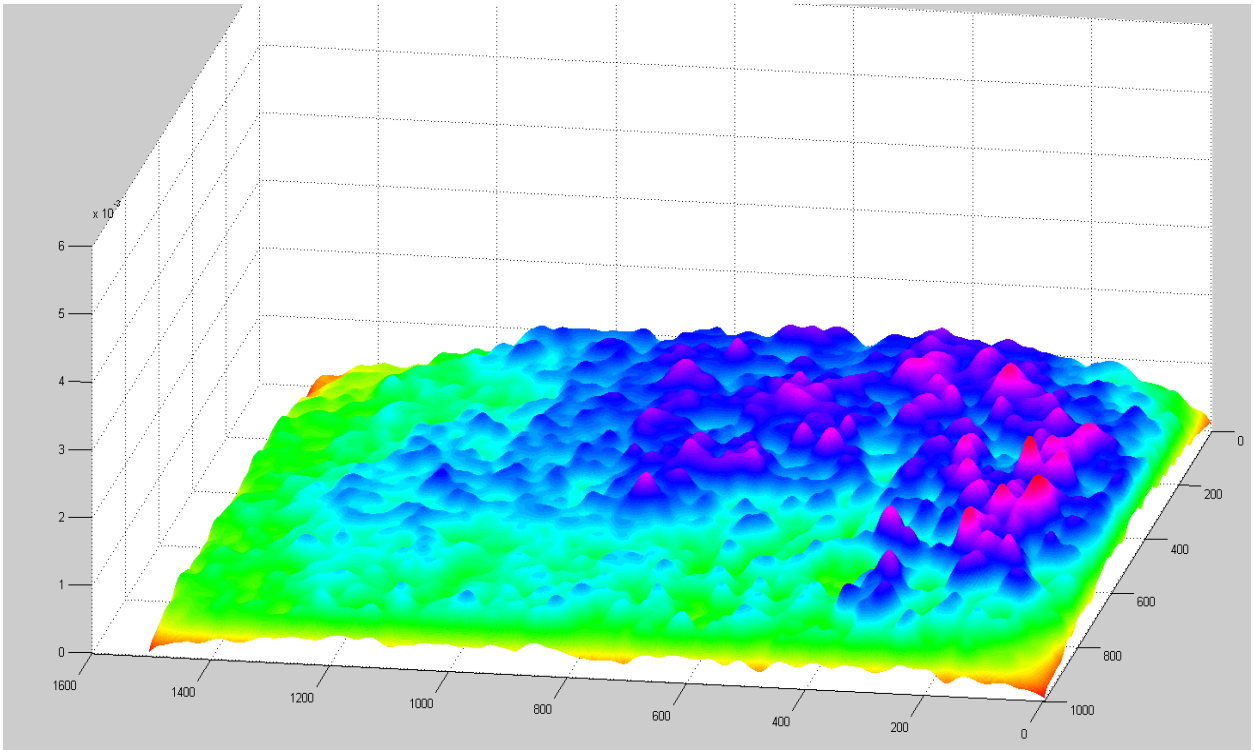

(c) SISA signature pattern of images in a normal vibrating system

Figure 3.2: Results of pseudo-random excitation in liquid vibrating system without any obstacle

In order to limit the order edges of the container the raw camera image as shown in Figure 3.2 (a) was focused on region of interest (ROI). Figure 3.2 (b) and (c) are the images obtained from the *SISA* processing. The data on the ensemble average in Figure 3.2 (b) shows that the perturbations were formed in middle and spreading out towards the edges of the system. Whereas the *SISA* signature in Figure 3.2 (c) shows the perturbations generated are evenly spread out throughout the space were observed at a magnitude less than 2×10^{-3}. Hence, it was concluded that in a fixed environment with proper lightening conditions, a threshold value of 2×10^{-3} was outlined to create a disparity between the normal and abnormal behavior of the system was accomplished.

In conclusion, the variable 'Sig (i, j)' for this case consisted solely of the noise component, with no information component, which is responsible for the presence of the abnormality from Equation (2.8). As there was no abnormality present, a uniform noise pattern was observed after the *SISA* processing. The idea behind processing the measured image from an active system without abnormality is that it is possible for us to predict on possible outcomes for the abnormal system depending on the obstacle, being finite or infinite impedance in nature, by examining the *SISA* signature pattern.

3.3.2 Pseudo-Random Excitation of Perforated Obstacle (Finite Impedance)

The second experiment was performed using an obstacle, which would simulate as a finite impedance that in this case was a perforated obstacle. Basic ideology behind the use of perforated obstacle was that most of the perturbations would be very small, as the obstacle is punctured with holes most of the vibrations will pass through it. This obstacle allowed us to understand the behaviour for submerged, loosely impeding abnormalities when the excitation is provided to the system. Due to the perforated nature of the obstacle the impedance created was finite, which means that instead of hindering all the wave excitation fed to the system, the finite impedance will hinder some part of the excitation. Logically, the perturbations created by this obstacle were assumed to be less than the infinite impedance obstacle. This experiment was a closer analogy towards the early abnormality as the smaller the perturbations, small perturbations are expected in incipient stages.

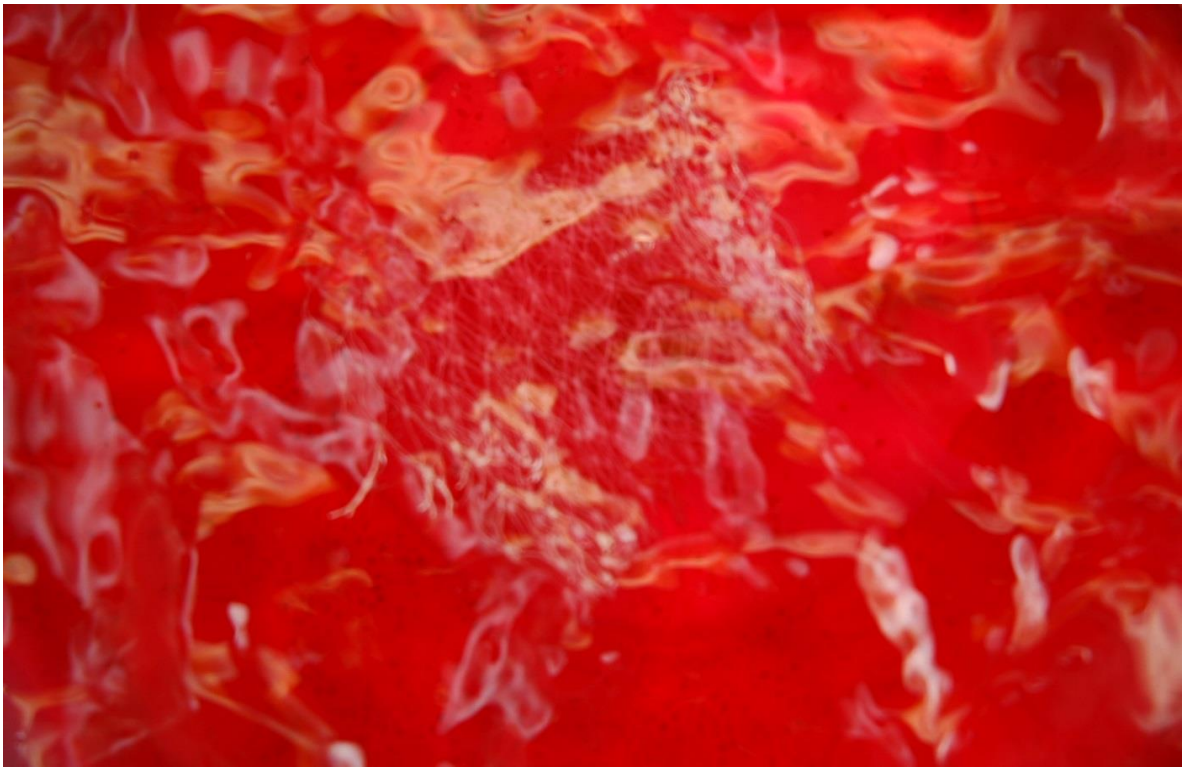

(a) Raw image of vibrating system with a perforated obstacle (finite impedance).

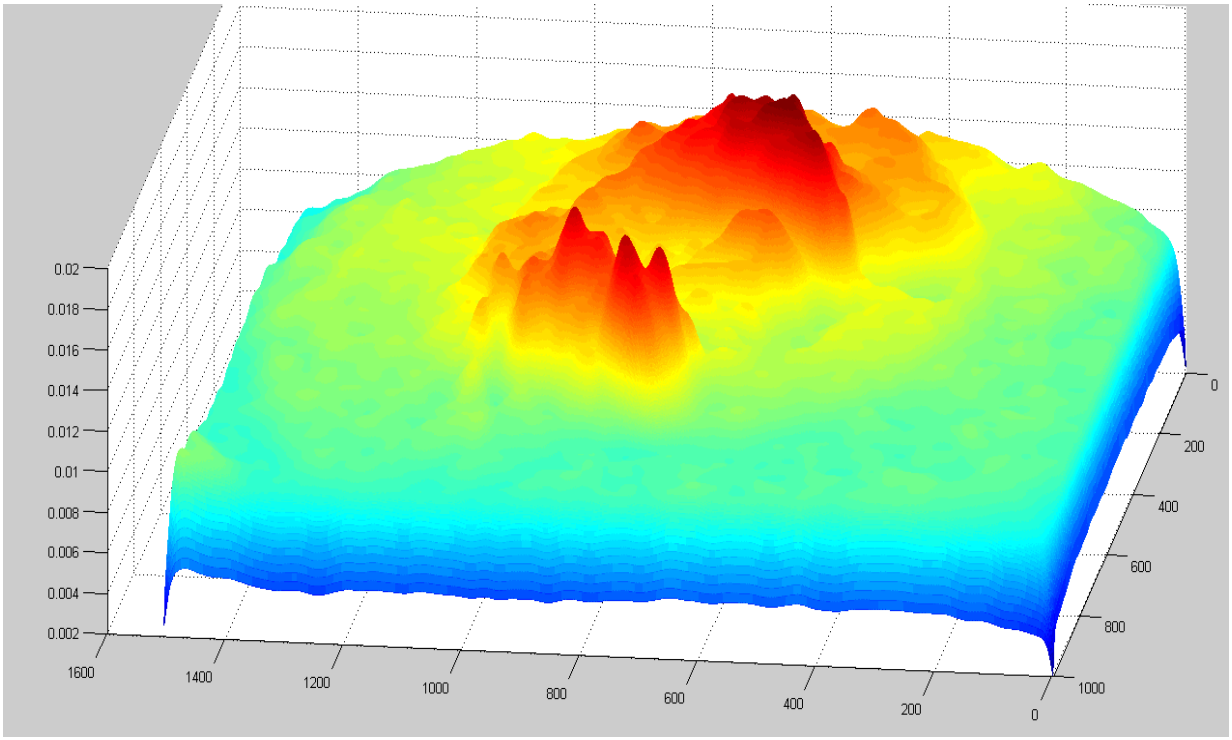

(b) Ensemble average of images with a perforated obstacle (finite impedance)

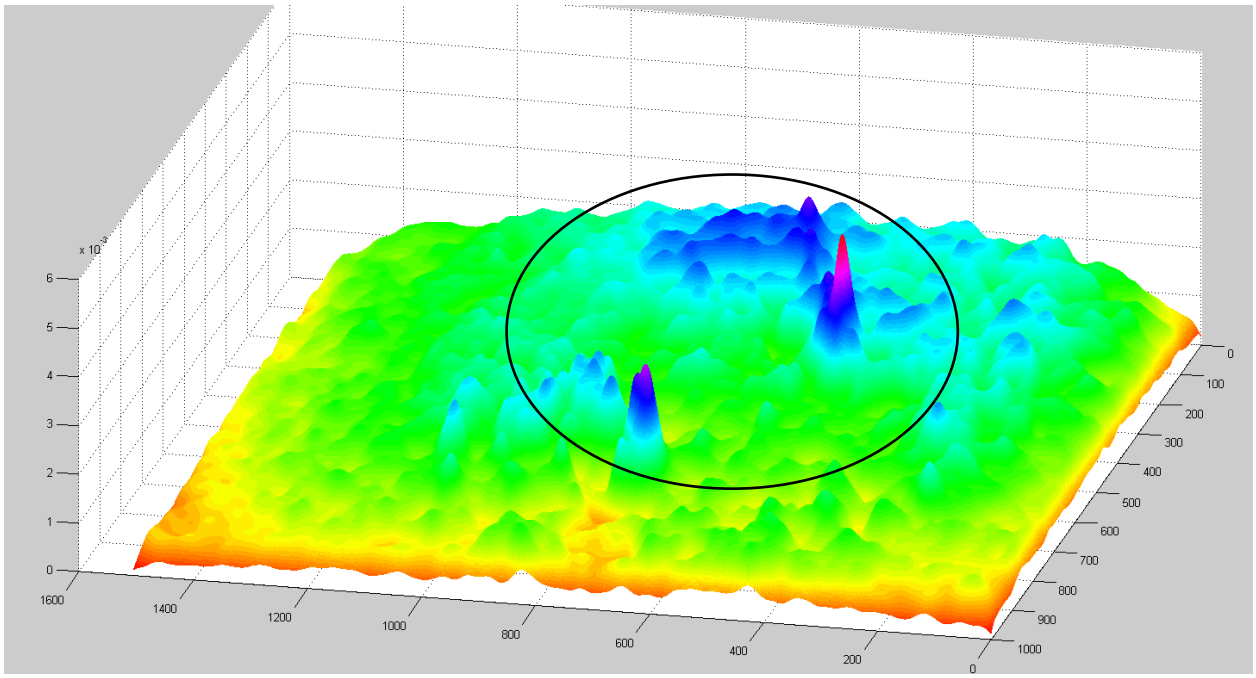

(c) SISA signature pattern of images with a perforated obstacle (finite impedance)

Figure 3.3: Results of pseudo-random excitation in liquid vibrating system with perforated obstacle of finite impedance

From the first image Figure 3.3 (a), the obstacle was submerged in the liquid, although some part of the obstacle was superficial to the surface and rest was inside. When pseudo-random excitation was fed to the setup, wave pattern as in Figure 3.3 (a) are observed. The results from this experiment were phenomenal that gave us a new insight about the behavior about the finite impedances.

In Figure 3.3 (b) and (c), the ensemble average and the signature pattern of a finite obstacle is shown, respectively. In Figure 3.3 (b), the shape of the obstacle can be clearly spotted that with the superficial part of the obstacle has high magnitude and submerged part has relatively low magnitude. In Figure 3.3 (c), the *SISA* pattern was observed, indicating the presence of an obstacle. It was observed that the higher perturbations were created from the superficial part as compared to the submerged part of the obstacle. The set threshold value of 2×10^{-3} from the previous experiment (in section 3.3.1), in this experiment much higher values on the *SISA* scale, were observed. The highest peak was about 5×10^{-3}, two times more than the threshold value, compared with the experiment 'without obstacle' for a finite impedance.

In conclusion, the *SISA* signature pattern was present with the information component, and it was clearly observed and deduced from the signature pattern, the nature and behavior of the obstacle. The obstacle had partial or finite impedance, as it is perforated in nature, and most of the vibrations passing through the obstacle; even then it would have created some perturbations due to its presence as compared with the normal system. As shown in Figure 3.3 (b), the possible shape and volume of the obstacle can be identified, but it is more precise from Figure 3.3 (c), the behavior of obstacle concluded from the *SISA* signature as finite impedance and it is positioned as partially superficial and partially submerged inside the solution.

3.3.3 Pseudo-Random Excitation of Solid Obstacle (Infinite Impedance)

In this experiment, use of infinite impedance was done using a solid obstacle (an iron bolt), the idea behind this choice of solid obstacle was to have an obstacle that can completely impede the pseudo-random excitation in the liquid. Therefore, instead of allowing the smooth flow of the pseudo-random excitation, the obstacle would create more perturbations due to its rigidity.

The idea behind this experiment was to understand the *SISA* signature pattern in the late stage in an active system, resembling a critical stage with a lot of problems in the system and has progressed to the final part of the disease, where the disease has long progressed from the early detection phase.

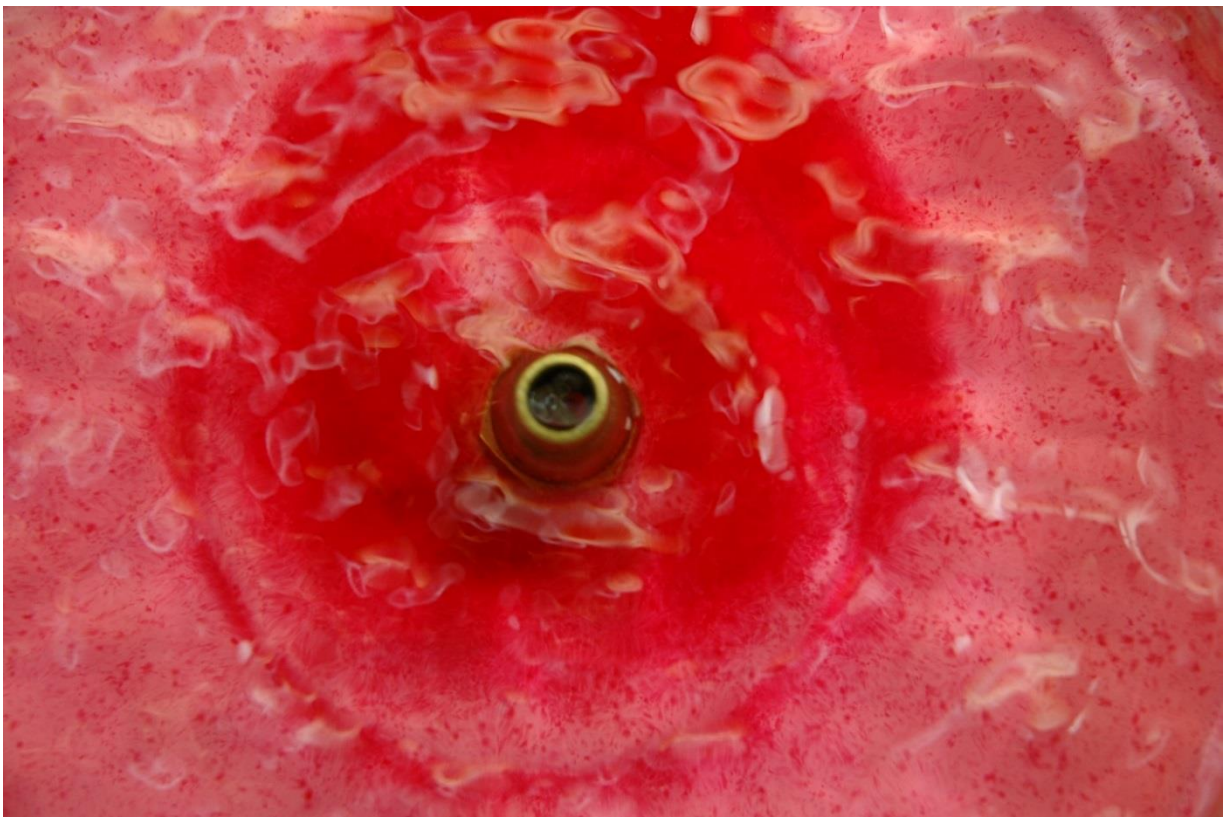

(a) Raw image of vibrating system with a solid obstacle (infinite impedance).

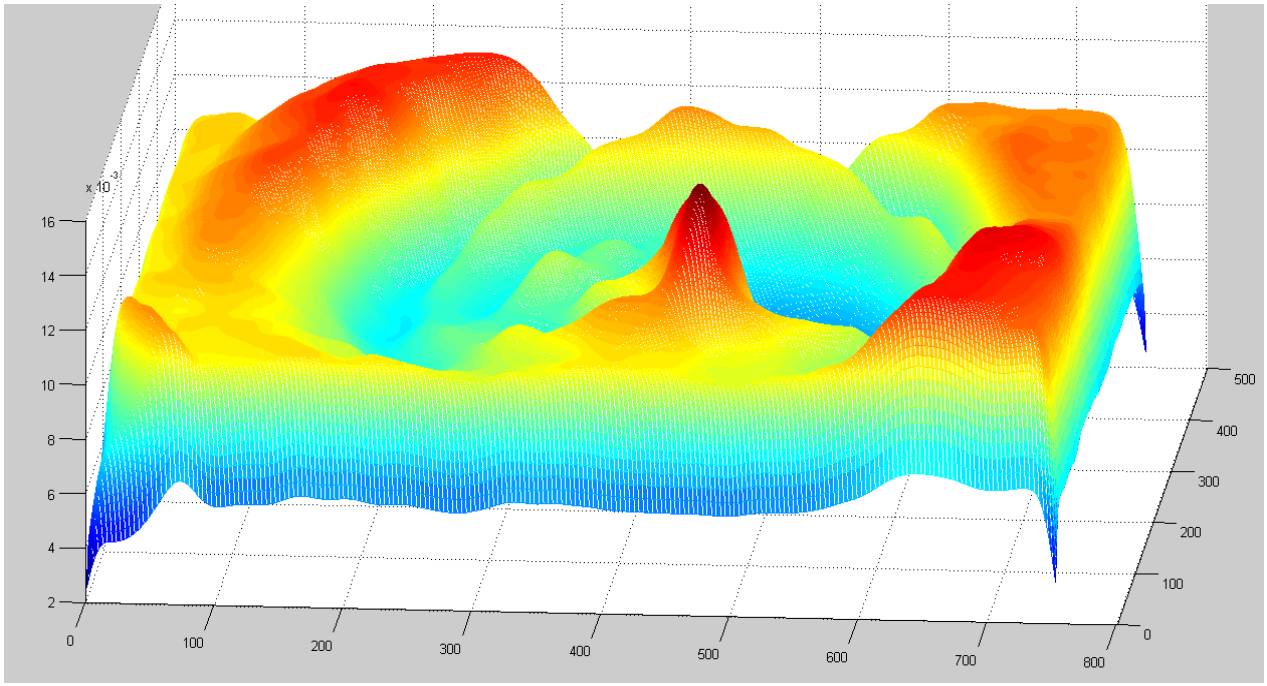

(b) Ensemble average of images with a solid obstacle (infinite impedance)

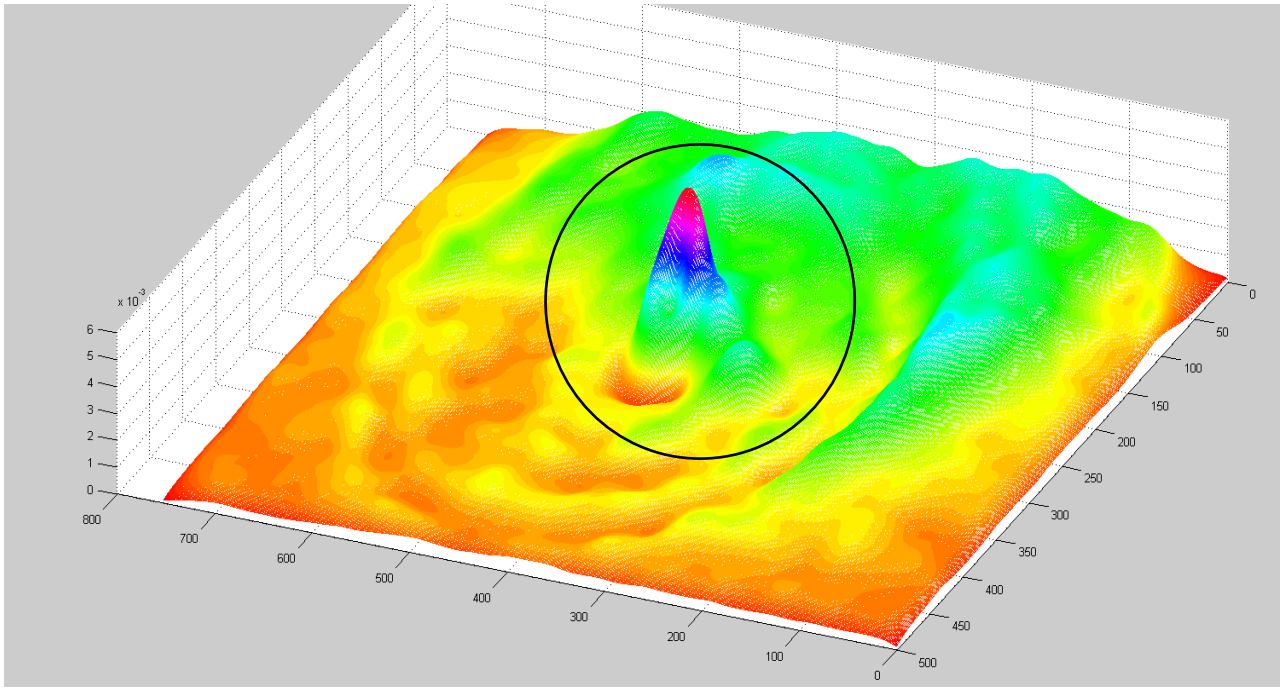

(c) SISA signature pattern of images with a solid obstacle (infinite impedance)

Figure 3.4: Results of pseudo-random excitation in liquid vibrating system with solid obstacle of infinite impedance

Figure 3.4 (a) shows the camera image, it was observable when the pseudo-random excitation was applied, high perturbations were bring created surrounding the region of interest close to the obstacle. In Figure 3.4 (b), the ensemble average of the measured image signal; the perturbation pattern was formed, due to obstacle impeding pseudo-random excitation in the container. The shape and the volume of the obstacle are being visible with the uniform pattern perturbation created by the obstacle. In Figure 3.4 (c), the *SISA* pattern highly distinguishable from the previous experiments, with a magnitude greater than 5×10^{-3}, which is three times more than the 'without any abnormality' experiment. Making it very likely to be detected and create higher perturbations using the *SISA* processing, concluding the disease has progressed from the early developing stages.

In conclusion, the solid obstacle was relatively inelastic and imperforated, unlike in the previous experiment and resembles infinite impedance; the behavior of infinite impedance was predictable as suggested in the mathematical formulation, with a large component of information in the *SISA* signature pattern. Infinite impedance was easily detectable, creating a large number of perturbations, which spread all around the region of interest uniformly. The infinite impedance represents an advanced stage, which impedes all smooth flows of excitation, like a tumor interacting with ultrasound. In this experiment, use of infinite impedance was done using a solid obstacle, the idea behind this choice and the approach was to have an obstacle that can impede the pseudo-random excitation in the liquid. Therefore, instead of allowing the smooth flow of the pseudo-random excitation, the obstacle would create more perturbations due to its rigidity.

3.3.4 Pseudo-Random Excitation of Two Solid Obstacles (Infinite Impedances)

In this experiment, two solid obstacles were used as infinite impedance, having two infinite impedances helped us understand the nature of one obstacle with respect to other, in terms of creating perturbations. Different from the previous experiment (in section 3.3.3), the solid obstacle on the left side in Figure 3.7 (a) was kept submerged in water and the other on the right was kept superficial to the surface in order to understand the wave pattern. Both the obstacles in this experiment were both rigid and perforated in nature, due to their hollow shape, different from the solid in the previous experiment. As shown in Figure 3.7 (a), the shape and size of the two obstacles were open and more susceptible to pseudo-random excitation, in terms of creating perturbations.

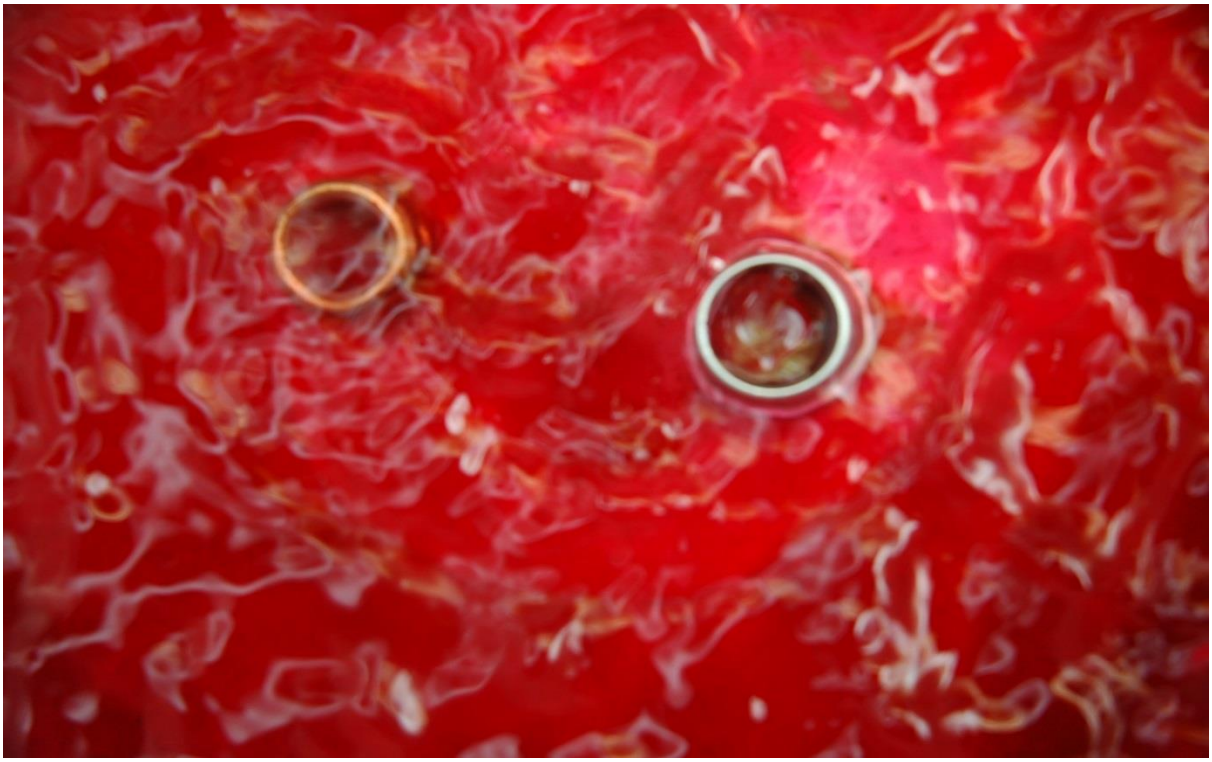

(a) Raw image of vibrating system with two solid obstacle (infinite impedances).

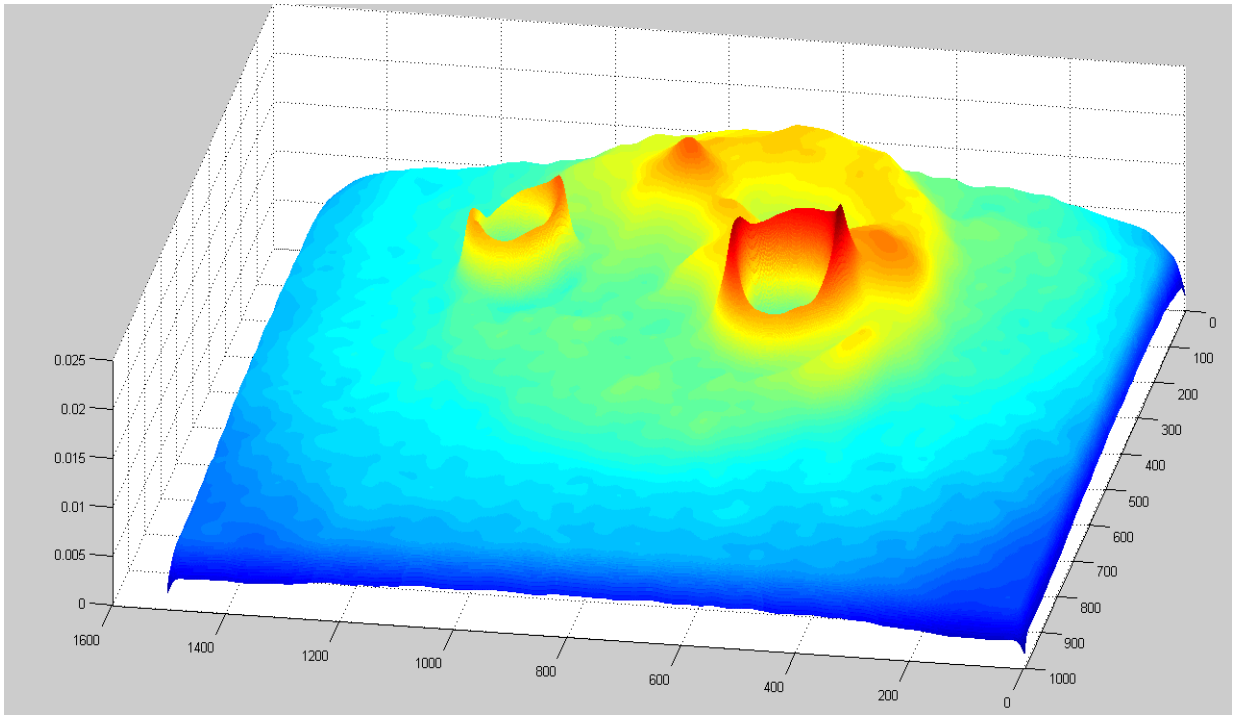

(b) Ensemble average of images with two infinite impedances.

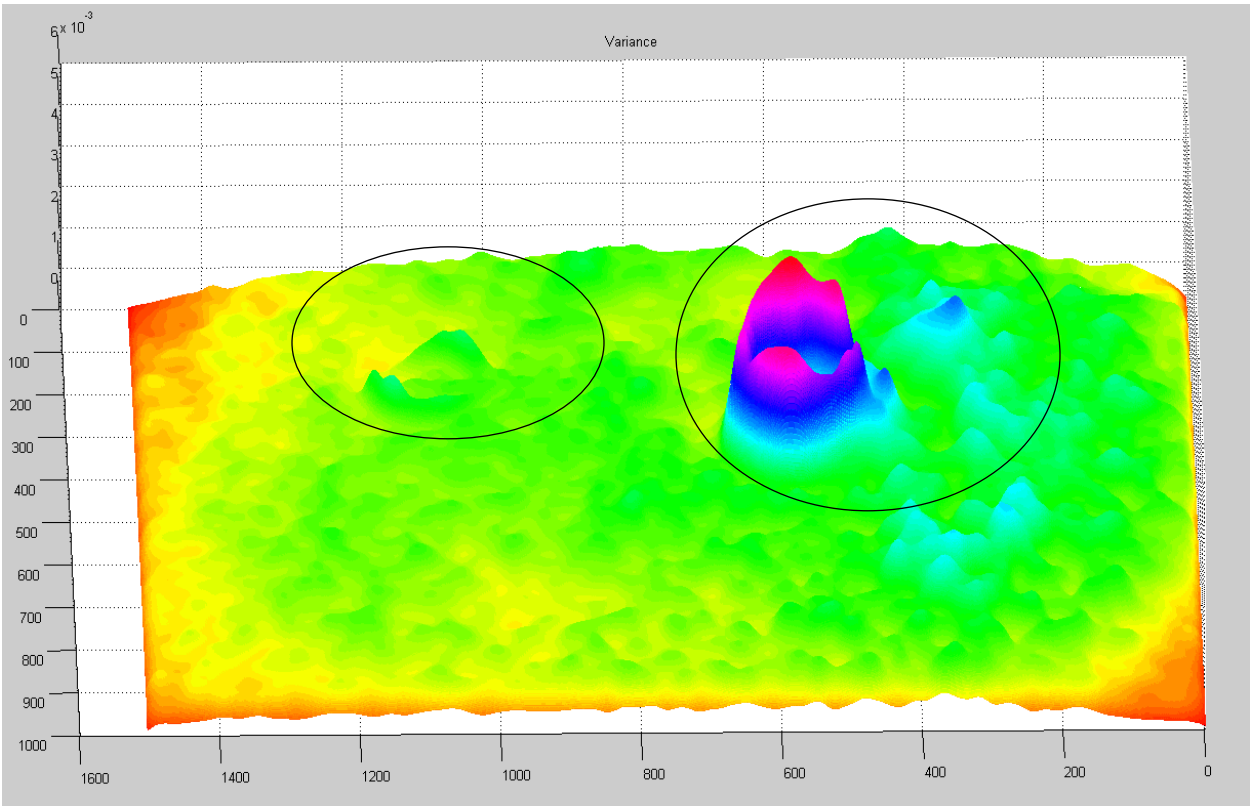

(c) SISA signature pattern of images with two solid obstacles (infinite impedances)

Figure 3.7: Results of pseudo-random excitation in liquid vibrating system with two solid obstacle (infinite impedances)

Two infinite impedances were positioned differently too, from Figure 3.7 (a), the obstacle on the right side (obstacle 1) of the images was kept superficial to the surface of the solution and the obstacle on the left (obstacle 2) was kept submerged in the solution. As it was observed from the experiment in section 3.3.2 that an obstacle behaves different when submerged in the solution. The same pattern was followed in this experiment, which can be observed in the processed images.

In Figure 3.7 (b), the shape of the obstacles is clearly identifiable. It was found that even though the obstacles had infinite impedance, their structure had a significant impact on the perturbations created by them. In Figure 3.7 (c), the *SISA* signature pattern is easily observable for the superficial obstacle (obstacle 1) creating high perturbations as compared with the submerged solid obstacle. In terms of magnitude on z-axis, obstacle 1 had magnitude greater than 3.5×10^{-3}, which is more magnitude than 'no obstacle' from section 3.3.1 and less than the infinite impedance 'solid obstacle' from section 3.3.3, obstacle 2 on the other hand, was different in behavior as expected from infinite obstacle due to its positioning, partial perforation and being submerged in liquid, in spite of that, the *SISA* signature pattern was greater than 2×10^{-3}, signifying a presence of abnormal behavior.

From the previous experiment in section 3.3.3, a similar perturbation pattern was observed in the perforated obstacle, the submerged part creating low magnitude on the *SISA* scale, in both of these cases, detection of the obstacle was succeeded. In conclusion, the behavior of obstacle 2 was different in terms of creating high-power magnitudes as expected in the observations from the previous experiment, the obstacle made a very significant difference in comparison with the normal active system. Whereas from this experiment it was determined that the abnormalities behave differently on the *SISA* pattern, when they are positioned differently

and other abnormalities are present to influencing each other. The information component (I_k), which is directly related to the nature of obstacle, was observed and measured with the use of *SISA* image processing technique.

3.4 Concluding Remarks

The liquid vibrating system experiment was the first step in implementing the *SISA* processing technique. The experimental results encouraged us to go further for ultrasound analysis. This experiment has also provided some basic understanding of detecting abnormality, followed by the idea that, if there is an abnormal behavior in an active system and some excitation is provided, extra perturbations are created by the abnormality. Based on these perturbations it is possible to detect the abnormality and conclude if the abnormality is in its early stages.

In the liquid vibrating experiment, in a circular container, with water-based solution, when an abnormalities or obstacles are introduced, some extra perturbations were created. While analyzing these wave perturbations, it was possible to detect these wave perturbations and evaluate further for identification. During this experiment, it was found that all abnormalities behave differently depending on their positioning, shapes and sizes.

When the obstacle was submerged completely, the wave perturbations pattern was different than obstacle on the surface. The intensity of these perturbations not only depends on the positioning but also the impedance of the obstacle. The non-linear impedance can be defined as the ability of the obstacle to restrict or hinder the smooth flow of activities in the system and create perturbations when excitation is provided to the system.

With the *SISA* technique, it was accomplished that with low (finite) impedance obstacle, the wave perturbations created were detected by the image processing. A low (finite) impedance

obstacle represents an abnormality in early stages, as the size and shape of abnormality is in its embryonic stage, which makes it harder to detect early signs of abnormality. Making this liquid vibrating system experiment, an analogy for an active system, the problems were detected and its various effects on the system were understood.

Chapter 4

FURTHER EXPERIMENTS ON TISSUES USING ULTRASOUND IMAGES

4.1 Ultrasound (US) - a brief introduction

Ultrasound (US) has been used to image the human body for around 50 years. Now, US is one of the most important, economic, widely used, and versatile imaging modalities in medicine [14]. Ultrasound imaging is a non-invasive technique and has many different types such as 2D or B-mode US, Contrast-Enhanced US, Doppler US, and they are used for different purposes In our study, 2D US (also known as B-mode US) was used.

Ultrasound uses a pulse-echo approach in which a small, localized pulse of ultrasound is produced by a device called transducer, which sends and receives the echoes directed towards it, as the pulse travels in the straight line along the tissue, [14, 15] as shown in Figure 4.1. The ultrasound beam, ideally, should be uniform travelling in a straight line, such as the laser, which could image the single line of tissue and the whole array of transducers would scan numerous images from that desired imaging spot. As the ideal condition can't be achieved in the case of sound waves, a method, called beam forming, closely relates to an ideal condition, where pulse

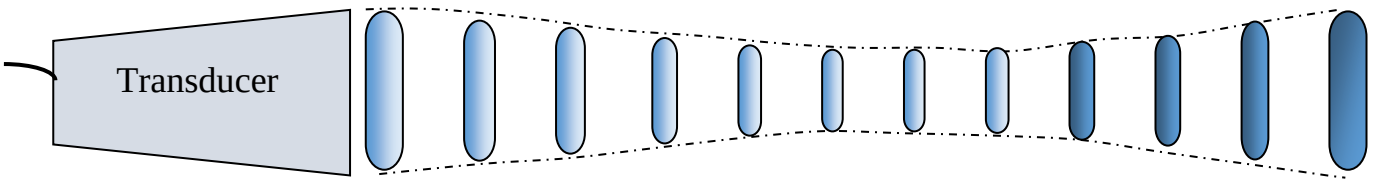

Ultrasound Probe

Figure 4.1: Focused ultrasound pulse wave pattern from the probe for better image scanning

generated is adjusted to make it as narrow as possible in the beginning and then becoming wider close to the imaging spot, for better imaging. Unlike, most of the waves travelling in a medium, US waves get reflected, refracted and absorbed, as they travel through it. The US probe measures the reflected waves using the piezo-electric principle and projects the image after calculating the intensity and the time taken for the wave.

Generally, a small segment of the ultrasound pulse is reflected back as an echo from any point in the patient, with the remainder of the pulse continuing along the beam line further and deeper inside the tissue. As the pulse travels deeper into the body, usually there will be long waves of echoes en route back towards the transducer, which is detected by the probe [15].

Ultrasound pulses travel through the tissues with different speeds depending on factors such as fat, muscle, liver, kidney and bone, with the average velocity of about 1.540 m/s [19]. Ultrasound pulses in the tissue medium contributes to the several specific types of interaction, one of which is the tissue property called acoustic impedance (Z), which is dependent on the density of the tissue (p) and average velocity (c) of ultrasound wave travelling inside the tissue; simply defined as, product of density of the tissue and the average velocity inside the tissue [14, 19],

Acoustic impedance is directly proportional to the density of the tissue and average velocity, which is given by

$$Z = p \times c \quad \ldots\ldots\ldots\ldots\ldots\ldots\ldots\ldots\ldots\ldots\ldots\ldots \quad (4.1)$$

To explore interactions of the ultrasound with the tissue, as in our experimental model, the abnormality taken from the respective tissue model was introduced again inside the animal tissue through an incision. Therefore, the final animal tissue for the experiment with the

abnormality will have impedance as (Z_1), and the dissected small tissue introduced from one part to another, relative to the surrounding will have impedance (Z_2). As both the impedance are derived from the same source, it can be concluded that the acoustic impedance will be, $Z_1 \approx Z_2$ [14, 19].

The intensity of the reflected echo increases with the increase of the impedance difference between the two tissues. In the case of tissues having almost identical impedances, which is a possibility in early stages, it results in less intense echo, and examining this over ultrasound gray-scale images can be difficult for the doctor to detect in the incipient stage. This makes a little challenging for the US, to detect and locate the small differences in the impedance. Ultrasound is a dynamic excitation technique, which induces vibrations, and maps the wave propagation throughout the tissue [19, 20]. US detects variations throughout the tissue, and with these variations in wave propagation helps in detection of the abnormality.

In 2D (or B-mode) US images, more reflective structures appear brighter than less reflective structures [14], more reflected structures meaning in B-mode that they reflect back more frequency determining their stiffness with respect to the surroundings, after all the backscattered echoes have been detected and processed, these signals are mapped to the proper locations in the pixel matrix, and the complete 2D image is shown on the US screen, the whole process is very fast and repeated immediately at the rate of about 20-40 frames per second.

The power density is generally less than 1 watt per square centimeter, to avoid heating and cavitation effects in the object under examination, which makes ultrasound a better non-invasive imaging technique without any long-term side effects [8]. Ultrasonic imaging applications include industrial non-destructive testing, quality control and medical uses [8].

In summary, the basic working principle of ultrasound can be understood as follows:

A) Ultrasound machine transmits a high frequency, ranging from 1 to 5 MHz, sound waves using a probe,

B) The sound waves travel inside the body and interact with the tissues, fluids and bones,

C) In this interaction, some of the sound waves get reflected, in the direction of the probe,

D) This process of interaction and reflection repeats travelling further deeper inside the body,

E) The reflected waves in the direction of probe are sent back to the ultrasound machine,

F) The machine calculates the distance from probe to the tissue, using the speed of sound in the tissue and the return time of the reflected wave,

G) The result is displayed with different intensities of the echoes or reflected waves on the screen forming a two-dimensional image for further analysis.

Ultrasound is a very promising choice, in non-invasive medical imaging techniques. It is economical, widely accepted, less time consuming, capable of taking large amounts of data. Ultrasound images, just as many other image modalities, are still poor for early detection, because they can only give the morphological information. [17, 18] Ultrasound being widely used and readily available for detection and diagnosis, it has been lagging behind in early abnormality detection, processing ultrasound images using *SISA* approach, it can provide a possible solution to this challenge. In this research, biological tissue samples from chicken and pig have been used to find the abnormality with *SISA* processing. Our experiment closely relates an abnormality in early stages because in imaging the tissue samples, a dissected sample from the respective tissue itself was used. In this section, we discussed how closely related change in impedance resemble

the ultrasound of tissue with respect to its surroundings. Therefore, it can be reasonably assumed that, with the use of part of the tissue as the abnormality itself pose as an early abnormality in the tissue.

4.2 Applications of Ultrasound Medical Imaging

In this section, some of the major applications are discussed ranging from cardiac muscles to kidney injuries. This section includes the details on ultrasound usage on different types of abnormal behavior in the human body. There are many applications of ultrasound, such as analyzing different types of tissues in the human body, which is helpful in detecting and locating the abnormalities as discussed below. *SISA* processing may be potentially useful in determining these abnormalities in the early stage of development. This section brings us closer to understand the use of ultrasound as a medical imaging associated with a diverse class of diseases. Ultrasound has been used in different studies as follows, in order to determine the cause and effects of the abnormalities.

Tumor perfusion

Perfusion in medical terms is known as the passage of fluid through the lymphatic system or blood vessels to an organ or a tissue. Tumor perfusion has a major problem recognized as a high importance in clinical and experimental cancers [21-23]. The use of contrast-enhanced ultrasound to assess tumor perfusion has been explored extensively in recent years [24]. Tumor perfusion has been recognized as an important problem in clinical and experimental cancers [25]. The study from Hoyt et al. has shown the possibility by development of real-time volumetric contrast-enhanced US (CEUS) imaging techniques to improve perfusion measurements [24, 26], which helps in understanding, not only the tumor behavior in the animal model but possible

detection for early tumor response using CEUS. Tumor perfusion heterogeneity has been demonstrated by more modest methods than CEUS, Doppler US [27, 29]. With this ultrasound technique perfusion rates in tumors and normal tissues have been able to determine the poorly perfused areas, distinguishable from blood perfusion in normal tissues and tumor [28, 29].

Chronic liver disease

Ultrasound in other studies has been proven to show chronic liver diseases such as fibrosis and cirrhosis [30]. Non-invasive methods for liver disease diagnosis have been developed in last decade. Instead of opting for painful liver biopsy, a non-invasive method to study the wound healing process of fibrosis can be observed from the US, with certain limitations to the model as the progression of the diseases with other liver diseases in consideration.

In another study, to identify the screening for significant liver diseases by comparing the ultrasound results in patients with chronic liver disease and liver biopsy in relevance to detection of fibrosis with patients under no pre-test suspicion of liver disease [31].

Breast cancer

Breast cancer remains one of the biggest cancer threats to Canadians. Over 22,000 Canadian women are diagnosed with breast cancer every year and one in nine Canadian women can expect to develop breast cancer in their lifetime [32]. A lot of research has been done in using different types of ultrasound such as elastography and color Doppler ultrasound as a better and easily accessible economic tool remains one step from detection and localization for early development stages of the tumor.

Benign thyroid nodules

With more technological advancement in ultrasound, the new body part can be used for imaging, e.g. benign thyroid nodules are comparatively quite recent, in detection using ultrasound. As the neck ultrasound is being popularized, the detection of growing number of asymptomatic thyroid nodules has been observed [33]. With a Fine-Needle Aspiration Biopsy (FNAB) – an invasive technique, being the best method to determine for differentiating benign from malignant thyroid nodules to treat the thyroid nodules. In order to select the patients, to undergo FNAB characteristics of gray-scale and Doppler ultrasound helps in the process [34, 35]. It is possible that ultrasound can be take one step further with the detection and localization of thyroid nodule, and the type of tumor can be analyzed using ultrasound imaging applications with *SISA* approach.

Acute kidney injury

Acute kidney injury (AKI) is a life-threatening disease involving the loss of kidney function and an increase in ischemia [36]. AKI is very controversial and has mortality rates approximately 50%. The treatment of the disease is directly related to progression and severity of it. Current methods include involvement of biomarkers for searching serum creatinine levels, lack sensitivity and specificity for early detection [37-39]. In the majority of the cases, renal US is the preferred imaging technique due to its availability, ease of use and safety [40].

Ultrasound is a great tool for imaging and research opportunities, using *SISA* approach we can understand these problems and detect them in their developing stages. From these various applications and worldwide research on ultrasound, it can be concluded that early detection and non-invasive imaging plays a major role in human health and *SISA* approach can play a vital role in this, with further experiments to bolster the technique. Following is the experimental setup and

results of the ultrasound analysis performed on chicken and pig tissues, in order to detect an abnormality.

4.3 Experimental Setup for Ultrasound Imaging

For ultrasound analysis, the experimental setup included 1) Tissue samples from pig and chicken, 2) Philips ultrasound machine, 3) Ultrasound probe and 4) Stand with a holder for the ultrasound probe. All samples were maintained at room temperature.

Tissue samples from pig and chicken

All measurements with the tissue samples were obtained at room temperature. The ultrasound frequency was pre-set to 5MHz. There were two types of measurements for each tissue sample - without any abnormality and with abnormality. As an abnormality, a small section of the dissected tissue was used respectively to each tissue sample. Additionally, a small tissue dissected part of the chicken tissue was used and introduced into the chicken tissue. Similarly, for the pig tissue, a small part of dissected pig tissue was used as the abnormality and was introduced inside the pig tissue.

Phillips Ultrasound machine

The ultrasound machine consisted of five main parts, namely:

1) Ultrasound probe: An ultrasound probe is the most important part of the ultrasound machine. The probe creates and receives the sound waves using the piezo-electric effect, as mentioned in section 4.1. In our experiment, GE C55 probe was used as an ultrasound probe.

2) *Processing unit (CPU):* Processing unit computes the raw data received from the probe and displays it with some other important information on the display screen. The CPU analyzes the intensity of the waves received and calculates the time taken for the sound waves to travel and reflect back, for the display.

3) *Display screen:* Display screen displays data processed by the CPU, depending on the type of ultrasound machine, the displays vary, but generally they are in black and white, showing the 3D image in a 2D plane.

4) *Keyboard control/ cursor:* During taking the measurements, the cursor can be used to make notes and estimate the distance between two given points. It also helps in controlling and changing the frequency and display types.

5) *Information storage*: Stores the patient's ultrasound scans for future medical records using CD, hard disks etc.

The duration of measurements was done for each experiment for about 15-22 seconds, at about 15 frames per second, at frequency of 5MHz. A total of 200 images were used to process in order to obtain the signature pattern. To keep the position of the probe fixed at a region of interest, the stand holder was used. The observations of normal behavior (no abnormality) of the tissue and the abnormal behavior (with abnormality) were made.

In the following section results of the ultrasound on animal tissue are discussed. All results consists of three main images, a) Direct image measured from the US machine, b) Ensemble average, c) *SISA* processed image also known as variance of the data, all of them are with and without abnormality mentioned separately.

4.4 Results of *SISA* Analysis using Ultrasound Images on Tissues

4.4.1 Experiment 1: Pig Tissue without any Abnormality

In this experiment, a pig tissue sample was analyzed using the ultrasound imaging. The sample examined first, is without any abnormality. The ultrasound image for a pig tissue model as shown in Figure 4.2 (a), was observed through the ultrasound machine. The measurements were taken on a fixed ROI, for both normal and abnormal cases. These observations were recorded, for further *SISA* processing, and after using the same methodology as for the liquid vibrating system, as discussed in section 2.2, the ensemble average of all the data recorded was retrieved, shown in Figure 4.2 (b).

(a) Ultrasound image of the pig sample model without any abnormality

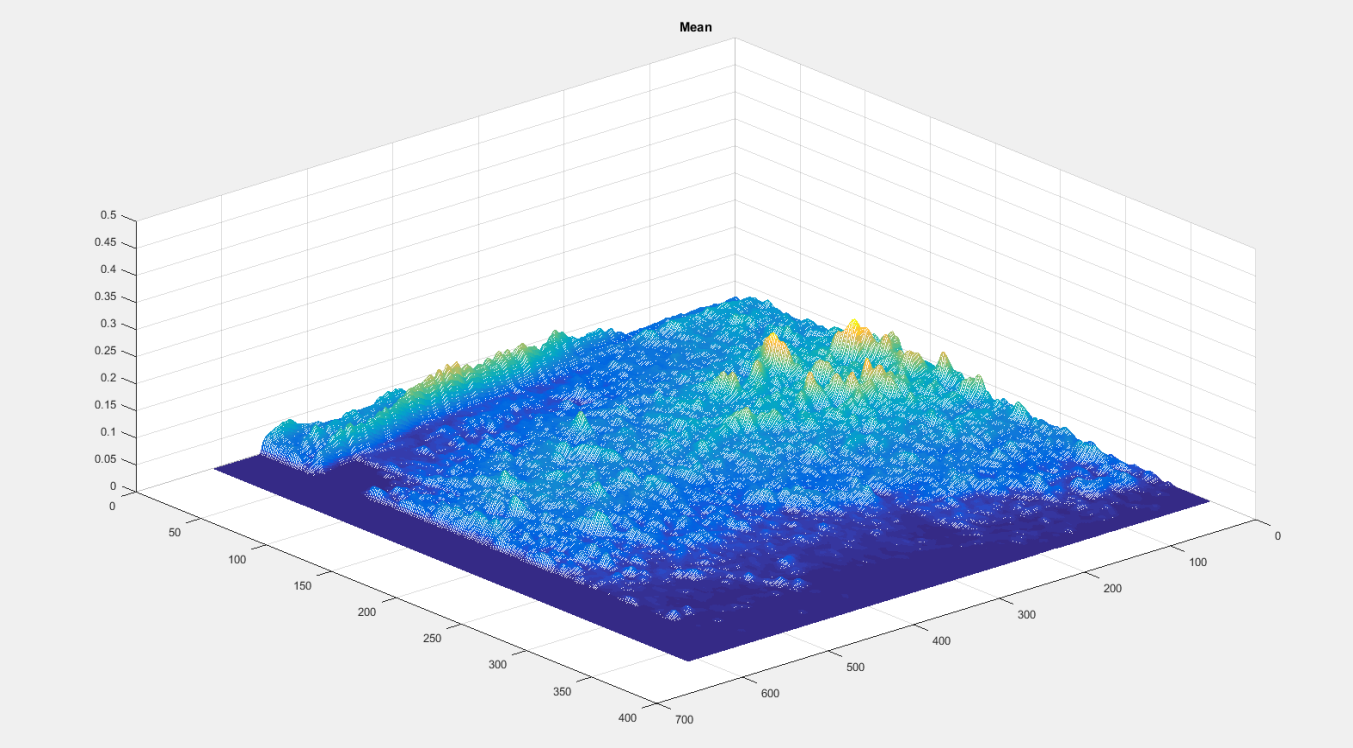

(b) Ensemble average of images of pig tissue without any abnormality

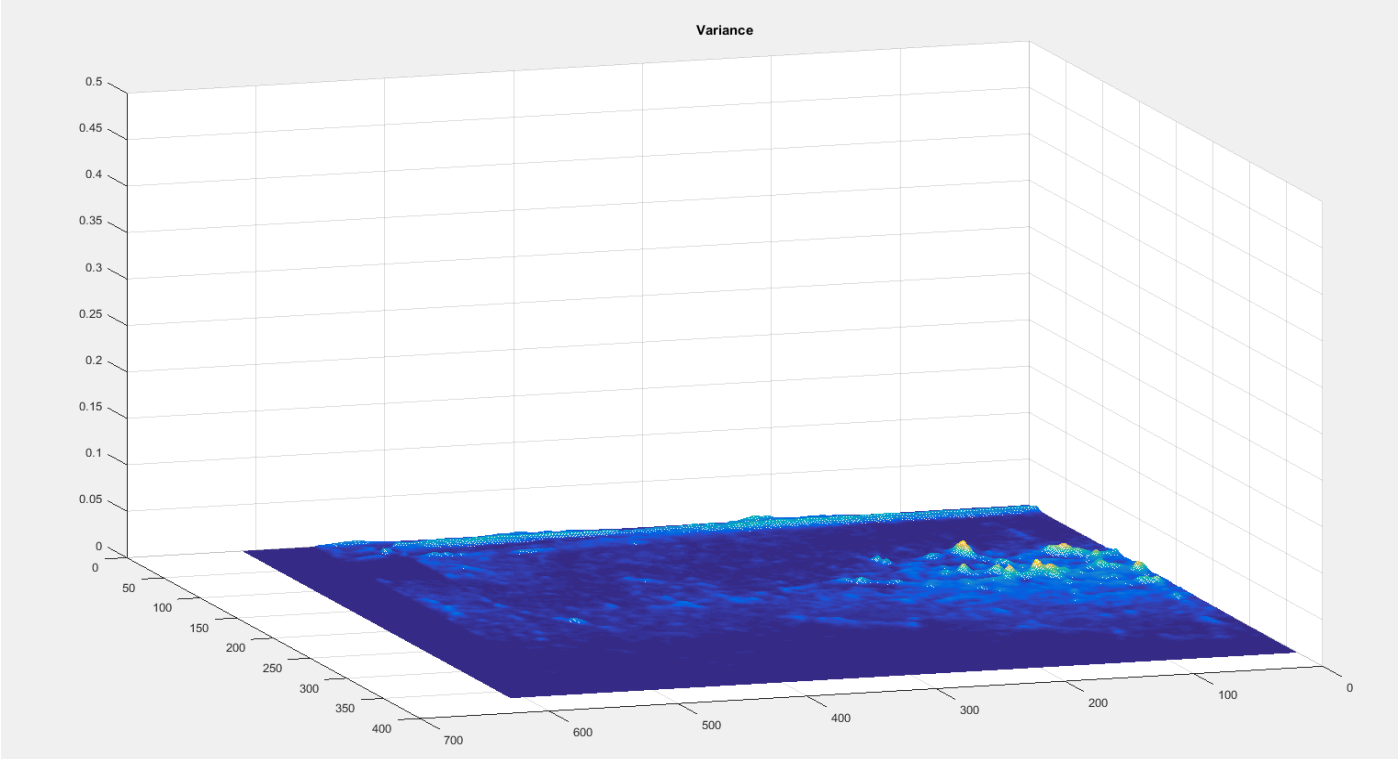

(c) SISA Signature pattern with no abnormality in the pig tissue

Figure 4.2: Results of ultrasound analysis of Experiment 1 in pig tissue without any abnormality

The *SISA* signature pattern was plotted as shown in Figure 4.2 (c), in order to define the threshold value and signify the presence of the abnormality in the tissue. From our experimental data, a threshold value was defined, which indicates that if the *SISA* signature pattern exceeds the threshold value, the presence of the abnormality can be confirmed, otherwise, if the *SISA* signature pattern doesn't exceed the threshold value, then it can be concluded, that no abnormality is present.

In Figure 4.2 (c), the *SISA* pattern with the magnitude on z-axis or *SISA* scale is approximately close to 0.01. The normal behavior of the sample helps us speculate the threshold value for creating the difference between normal and abnormal behaviors. Hence, from this experiment, it can be determined that in a pig tissue sample if the *SISA* scale has more than 0.01, the presence of abnormality can be concluded. The abnormality is more appropriately used in the medical imaging area, whereas in obstacle was a relevant choice for something with impedes the smooth flow of the vibrations, in order to avoid confusion.

In conclusion, for this experiment 1 with pig tissue the *SISA* signature pattern or the variance, in Figure 4.2 (c), had no information component, and the remaining noise component was uniformly distributed all over the fixed space. Overall, the variance was evenly spread to 0.01, therefore, we can speculate that in case of abnormal behavior the variance should be much more than the value observed in normal pig tissue sample

4.4.2 Experiment 2: Pig Tissue with an Abnormality

In this experiment, an abnormality was introduced in the pig tissue sample, it was introduced through a side incision around the region of interest. Figure 4.3 (a) shows the ultrasound machine display, which was observed with the abnormality present. After processing the images obtained from the measurements, the *SISA* technique could identify the gray-scale image from ultrasound and be able to locate the abnormal behavior.

Figure 4.3 (b) illustrates the ensemble average of all the measured images in the pig tissue with the abnormality, with a rough shape of the abnormality present inside the sample. Figure 4.3 (c) shows the variance or the *SISA* signature pattern of the pig tissue with the highest magnitude of about 0.45 on the *SISA* scale. This shows us the tremendous difference in the between the normal and the abnormal behavior using *SISA* technique.

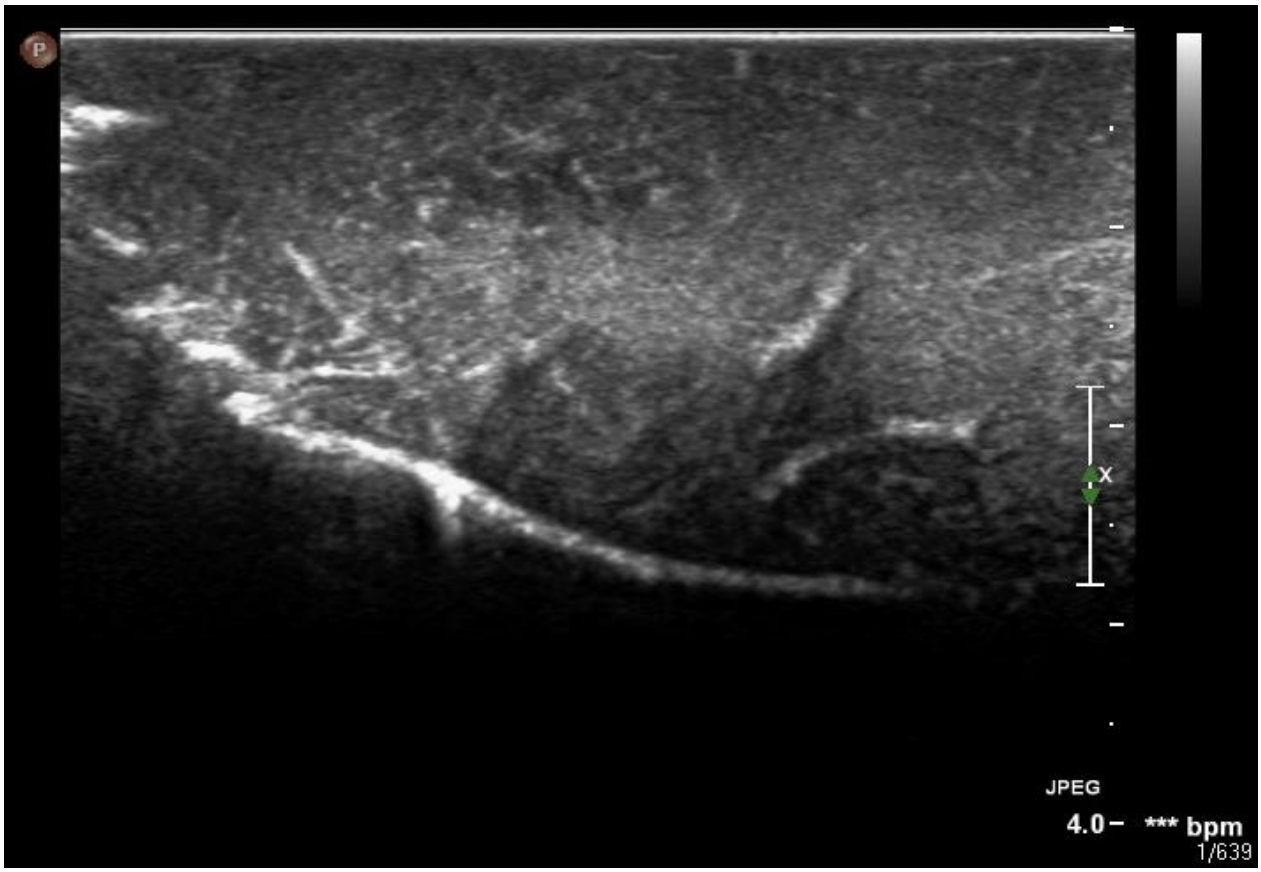

(a) Ultrasound image of the pig sample model with abnormality

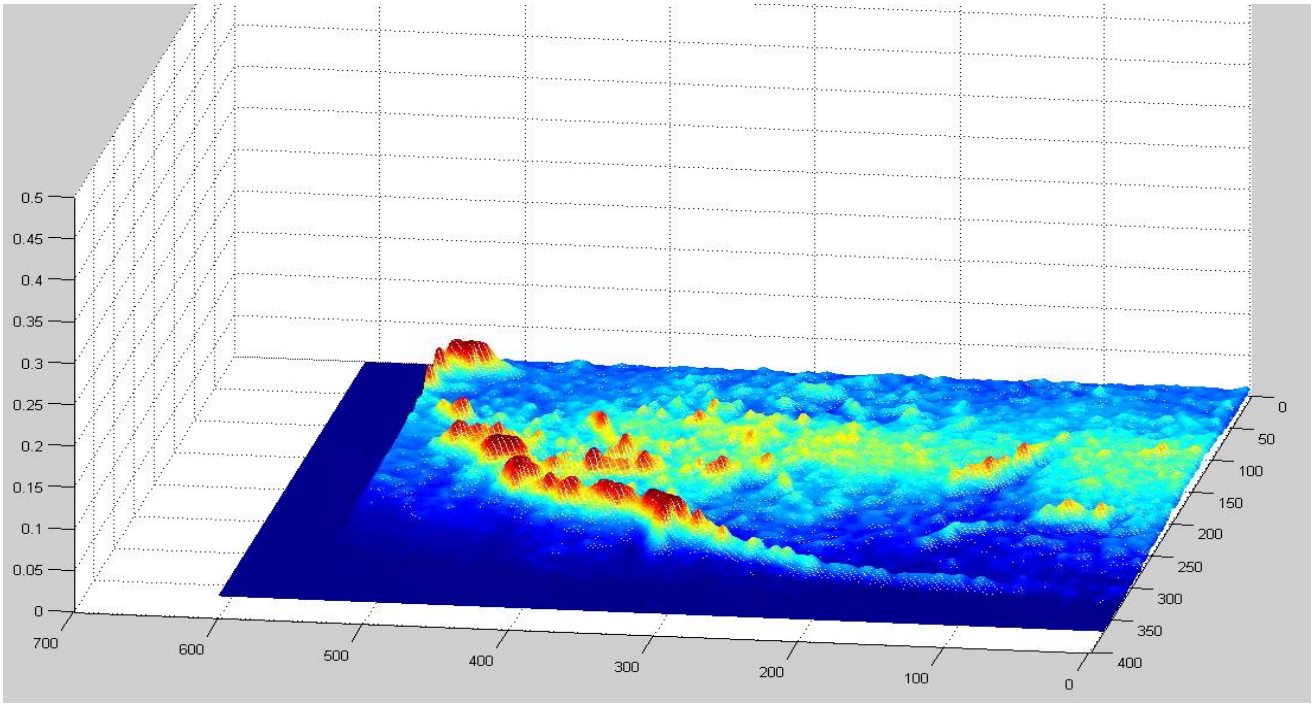

(b) Ensemble average of images of pig tissue with abnormality

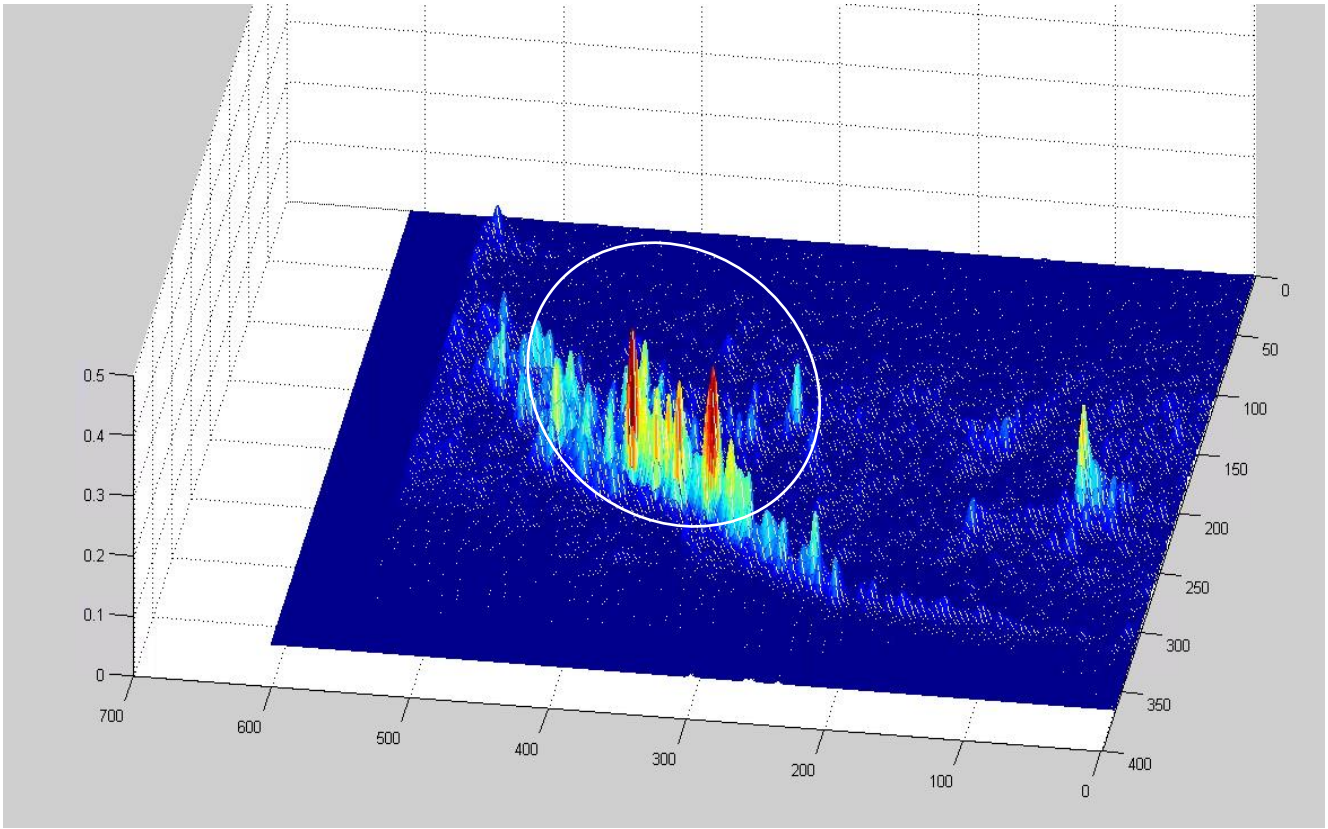

(c) SISA Signature pattern with abnormality in the pig tissue

Figure 4.3: Results of ultrasound analysis of Experiment 2 in pig tissue with an abnormality

In conclusion, the abnormality was located and the vast difference in the variance in the pig tissue sample without abnormality from section 4.4.1, as compared with presence of abnormality, in the *SISA* signature pattern in Figure 4.3 (c) was observed. Around the same region of interest the abnormal behavior changes and the information component generated by the abnormality from the mathematical formulation in section 2.2.1 is much higher and significant.

4.4.3 Experiment 3: Pig Tissue without any Abnormality

The experiment 3 under similar conditions using pig tissues was very consistent as the previous ones. To obtain a set value for determining the true abnormal behavior from normal behavior in the active system, more analysis was required. This experiment was conducted to establish the foundation for *SISA* signature pattern. For this experiment another pig tissue sample was taken and was imaged using ultrasound machine under similar conditions to obtain similar results. Figure 4.4 (a) shows the pattern can be observed and this sample was different than the one in experiment 1, with difference in tissue texture.

After imaging and recording the data from a randomly chosen fixed region of interest. For further *SISA* analysis, using same approach in previous experiment was done.

Figure 4.4 (c), shows no significant change in the variance of the graph. As there is no information component due to the absence of any abnormal activity, the signature pattern is space-invariant, as it consists of solely noise component, which is evenly distributed around the plane. Except for the few small random peaks in the graph, nothing significant is observed in the signature pattern, suggesting the pig tissue model was better to study model for analysis of medical imaging in the biological system.

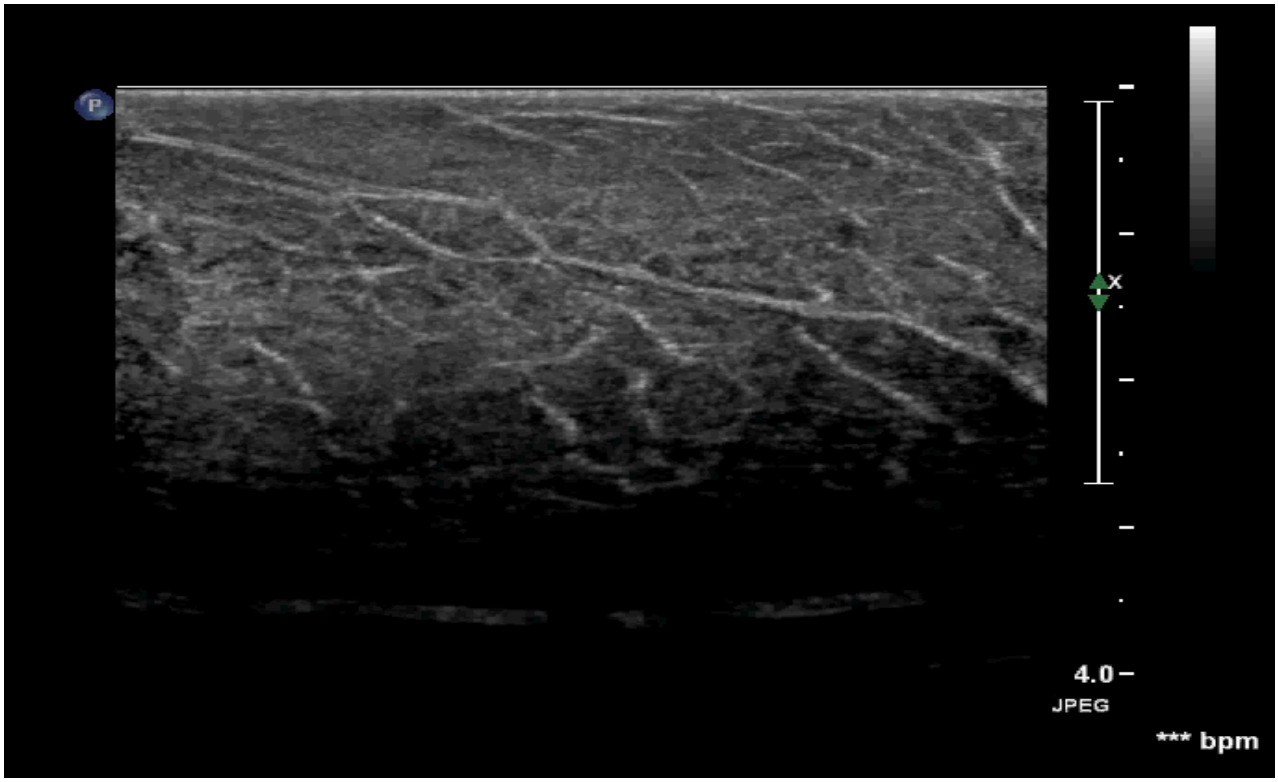

(a) Ultrasound image in experiment 3 of pig sample model without any abnormality

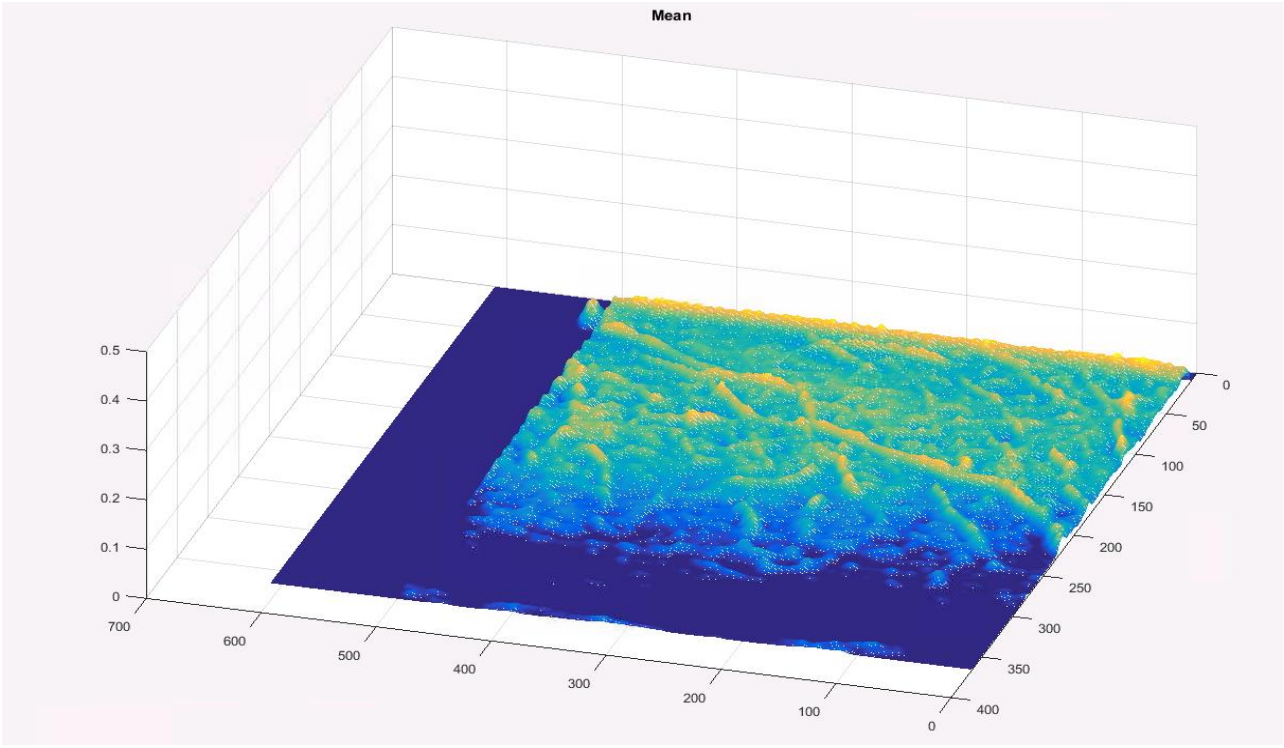

(b) Ensemble average in experiment 3 of pig sample without any abnormality

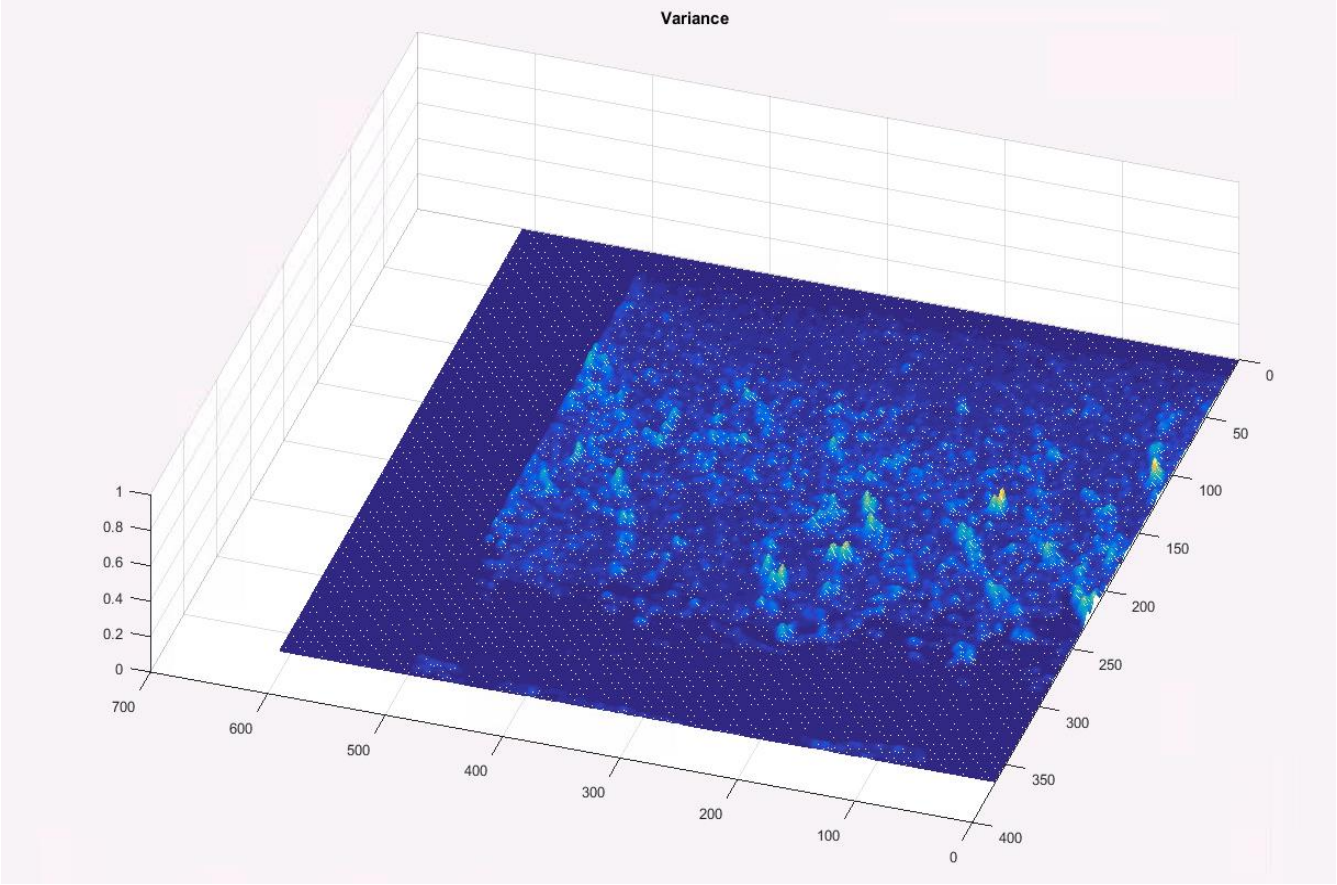

(c) SISA signature pattern in Experiment 3 of pig sample model without any abnormality

Figure 4.4: Results of ultrasound analysis of Experiment 3 in pig tissue model without any abnormality

In conclusion, both the experiment with different pig tissue samples were successful. The *SISA* signature pattern had some random peaks around the graph but was not significant. In terms of both size and the magnitude on the z-axis, hence, it can be assumed the noise component was evenly spread across the whole region of interest in Figure 4.4 (c).

The *SISA* signature pattern didn't exceed the value of 0.1, in both cases of normal behavior in pig tissue samples. It can be summarized that for an abnormal behavior to show in *SISA* signature pattern, the volume should be more and the magnitude should be larger than 0.1

on the z-axis. However more experiments are required in similar conditions, to bolster the threshold value.

4.4.4 Experiment 4: Pig Tissue with an Abnormality

This experiment is very similar to the earlier one, and for experiment 4, the same conditions as experiment 2 were maintained. The abnormality was dissected from the pig tissue sample and stuffed inside around the region of interest. The ultrasound probe was kept fixed using stand holder on the ROI and the measurements were made. The ultrasound image in Figure 4.5 (a) with an abnormality in the pig tissue sample was observed. Figure 4.5 (b) shows the ensemble average of the measured images. As shown in Figure 4.5 (c) *SISA* signature was clearly able to distinguish the abnormal behavior in the region of interest.

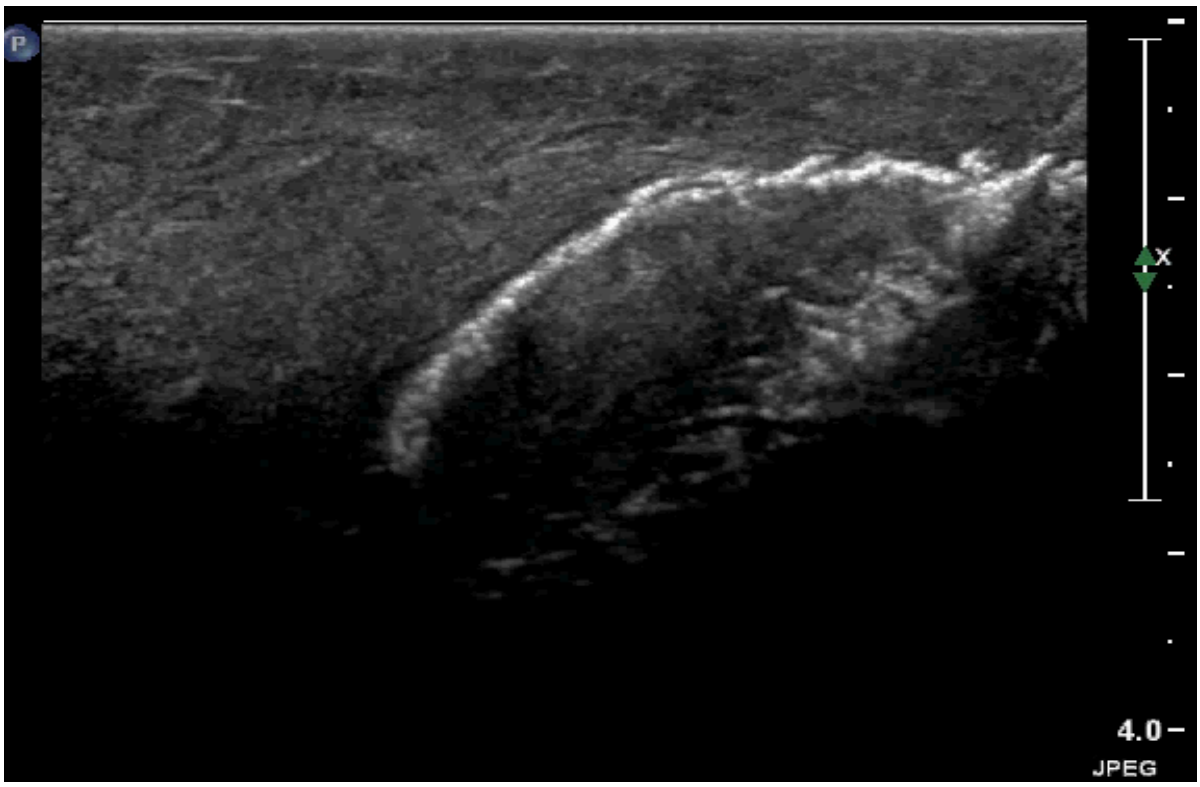

(a) Ultrasound image from Experiment 2 of pig sample model with abnormality

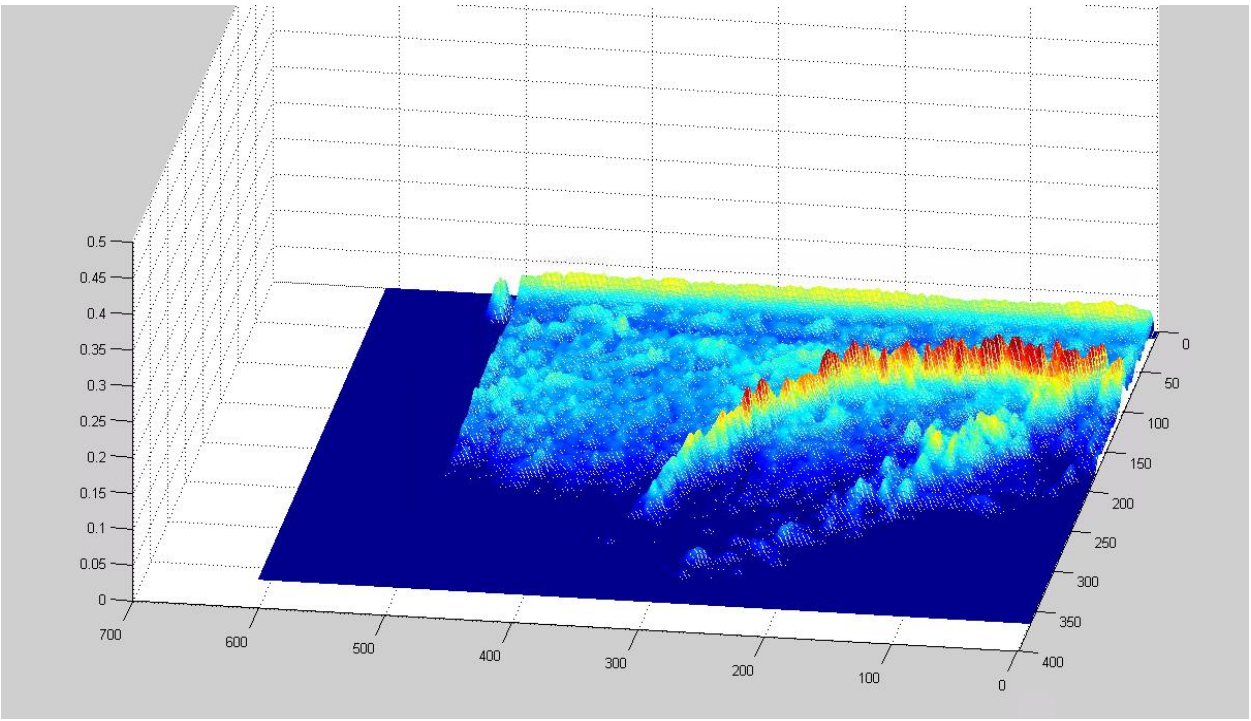

(b) Ensemble average from Experiment 2 of pig sample model with abnormality

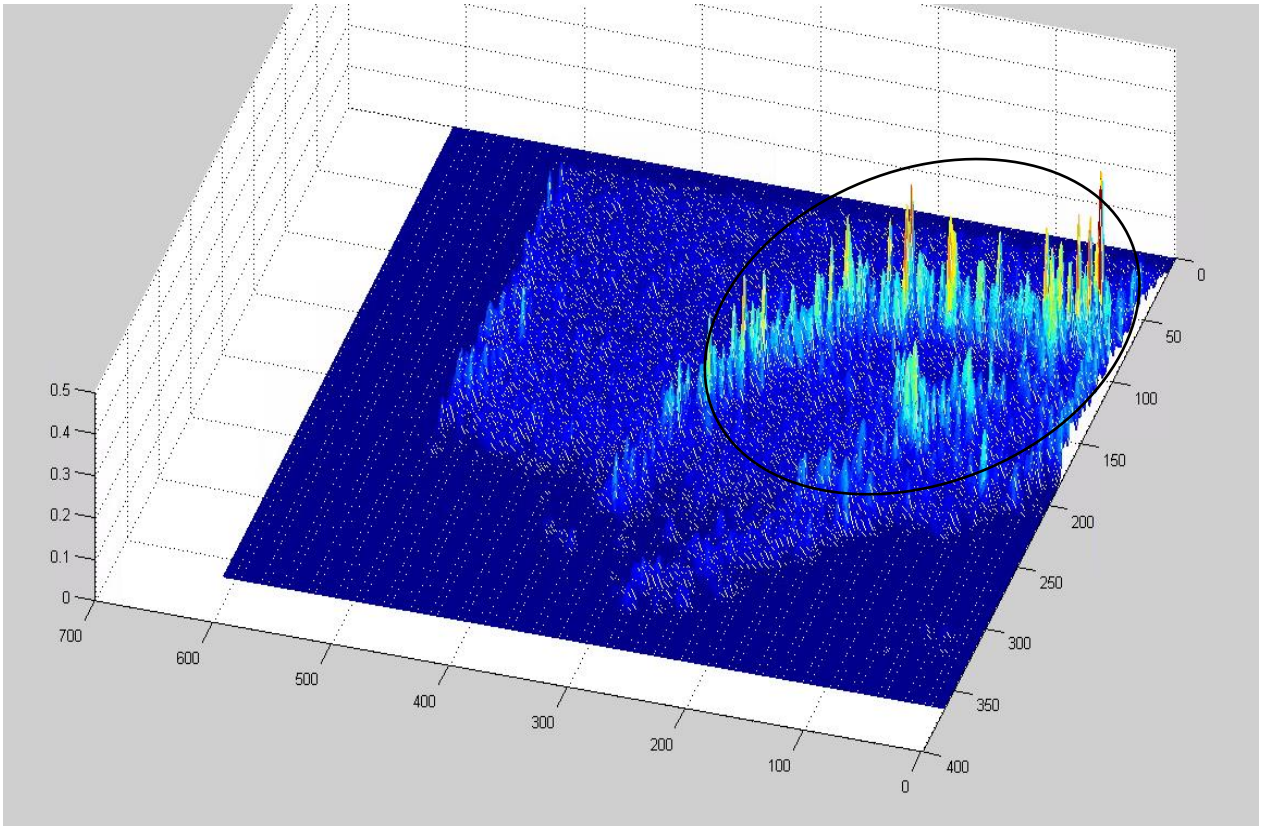

(c) SISA signature pattern from Experiment 2 of pig sample model with abnormality

Figure 4.5: Results of ultrasound analysis of Experiment 2 in pig tissue with an abnormality

It was clearly observable that the position and the shape of the abnormality, and it is very different from the previous experiment under measuring conditions, as discussed in section 4.1, the ultrasound waves travels in the medium and interact with different layers of the tissues, the sound waves are reflected back at the probe. From the Figure 4.5 (c), the signature pattern with the ability to detect and process this interaction in the tissue and help locate the abnormality.

In conclusion, the pig tissue sample was the good choice of model for studying and understanding the ultrasound and *SISA* processing in a biological system. The *SISA* technique was able to detect and localize the abnormality. With a few experiments, there was an inclination in determining the threshold value for easily locating and detecting abnormal behavior in the tissues, which is very important in early detection, as most of the cases go unnoticed until they progress to later stages.

4.4.5 Experiment 5: Chicken Tissue without any Abnormality

For ultrasound analysis, alongside the pig tissue, chicken tissue model was used. The need for another type of tissue model was necessary to observe the difference generated in the *SISA* signature pattern. Chicken tissue was comparatively thinner and had a different tissue texture and density than the pig. Figure 4.6 (a) is the raw ultrasound image while recording the data. Further, measurements were taken on fixed region of interest, similar to chicken and pig samples. The observations were recorded for about 15-17 seconds, and the frames from the ultrasound video were processed to obtain the *SISA* signature pattern. Figure 4.6 (b) and Figure 4.6 (c) are the processed image of ensemble average of ultrasound images and signature pattern respectively. From Figure 4.6 (c), the overall *SISA* scale on z-axis value didn't exceed 0.05, and the signature pattern was uniformly distributed when the abnormality is not present. This creates

difference in *SISA* scale in terms of different tissue types, which is expected as the ultrasound waves depends on density of the tissue and the average velocity inside the tissue.

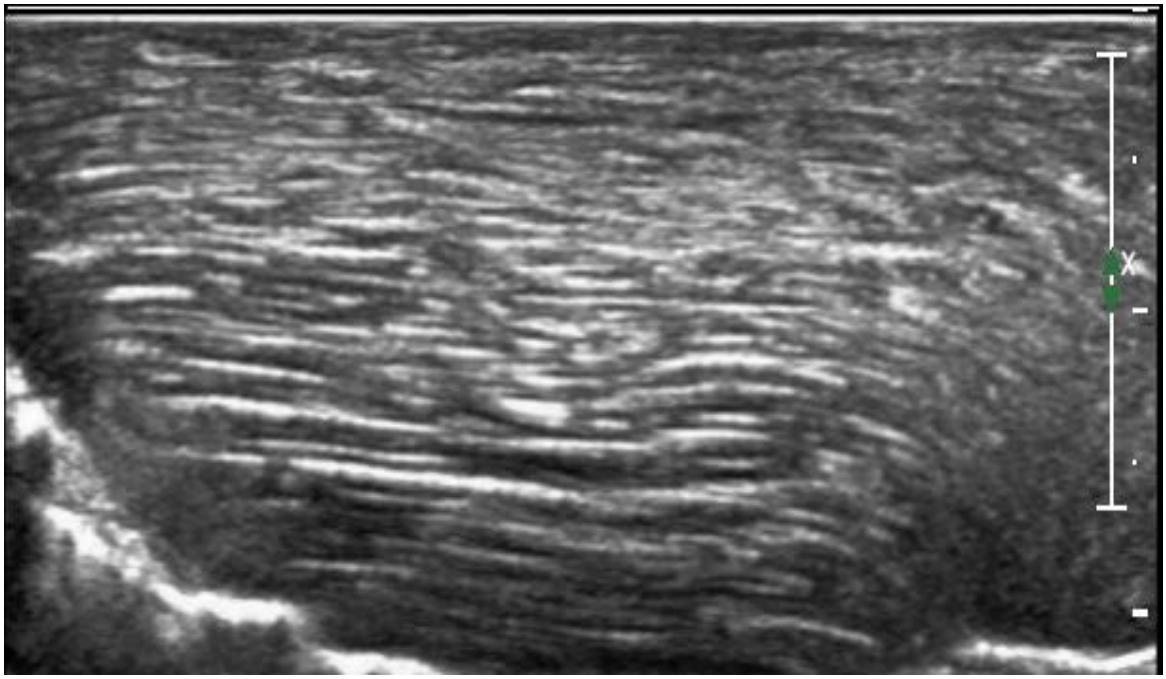

(a) Ultrasound image of chicken sample model

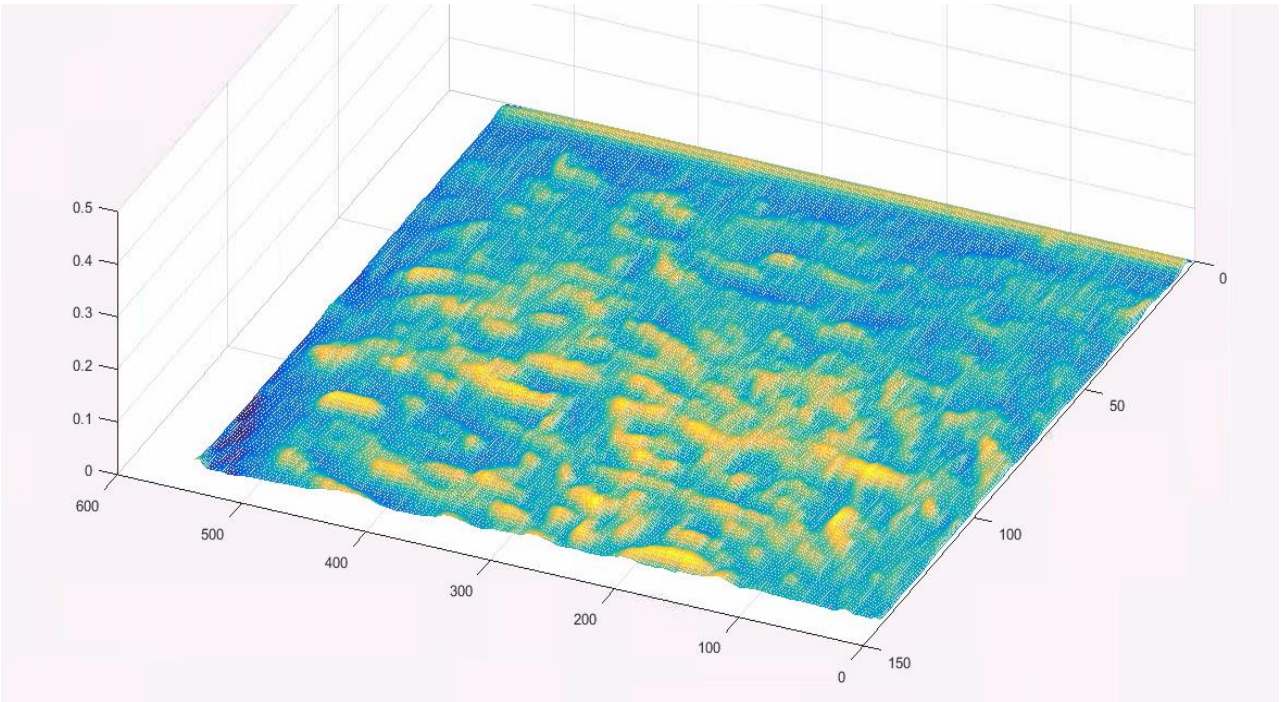

(b) Ensemble average of chicken sample without abnormality

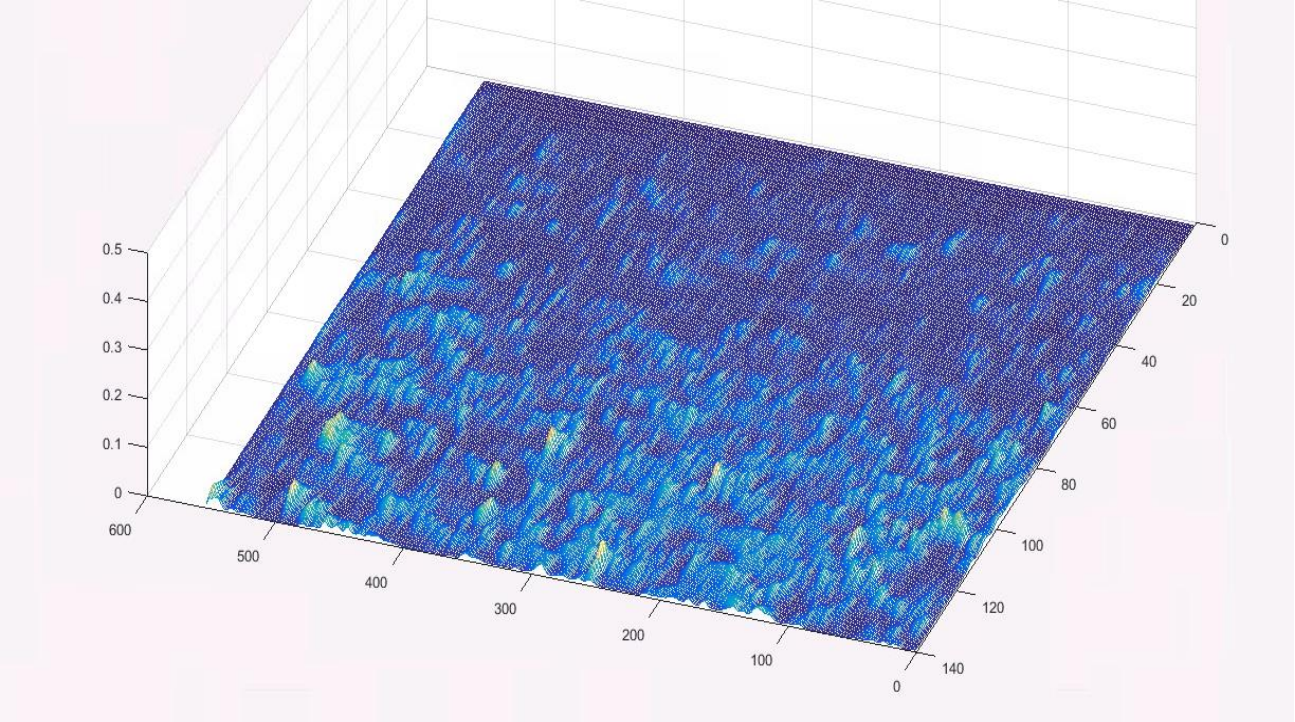

(c) SISA Signature pattern without any abnormality in the chicken tissue

Figure 4.6: Results of ultrasound analysis in Experiment 5 in chicken tissue without any abnormality

In short, the chicken tissue without any abnormality had a different texture of tissue as compared to pig tissue. Under similar conditions, a normal signature pattern for chicken tissue model, in Figure 4.6 (c), had no information component, as the abnormality was absent, but the signature pattern consist of space-variant, because of ultrasound waves reflecting surface, in a normal chicken tissue model.

Therefore, from this experiment it can be concluded that different type of tissue structure can form a different signature pattern, as every tissue type is different and each layer of tissue, bone and fluids inside a biological system such as human body can be very complex and challenging. Various organs inside the human body are made with different compact densities and will create different *SISA* pattern for each of them, using ultrasound imaging, it is required to

image the tissue to understand the pattern under normal and abnormal circumstances using *SISA* approach.

4.4.6 Experiment 6: Chicken tissue with an Abnormality

In this experiment, an abnormality was introduced to the previous chicken tissue model, similar to previous experiments; the abnormality was derived from the dissected part of the tissue itself, and was introduced in the region of interest. The region of interest was kept fixed for both with and without abnormality experiments, for consistency in measurements. From the following images, the raw ultrasound image with the abnormality, which can be observed on the right top of the image in Figure 4.7 (a). Figure 4.7 (b) and (c) are the ensemble average of all the images and *SISA* signature pattern, respectively.

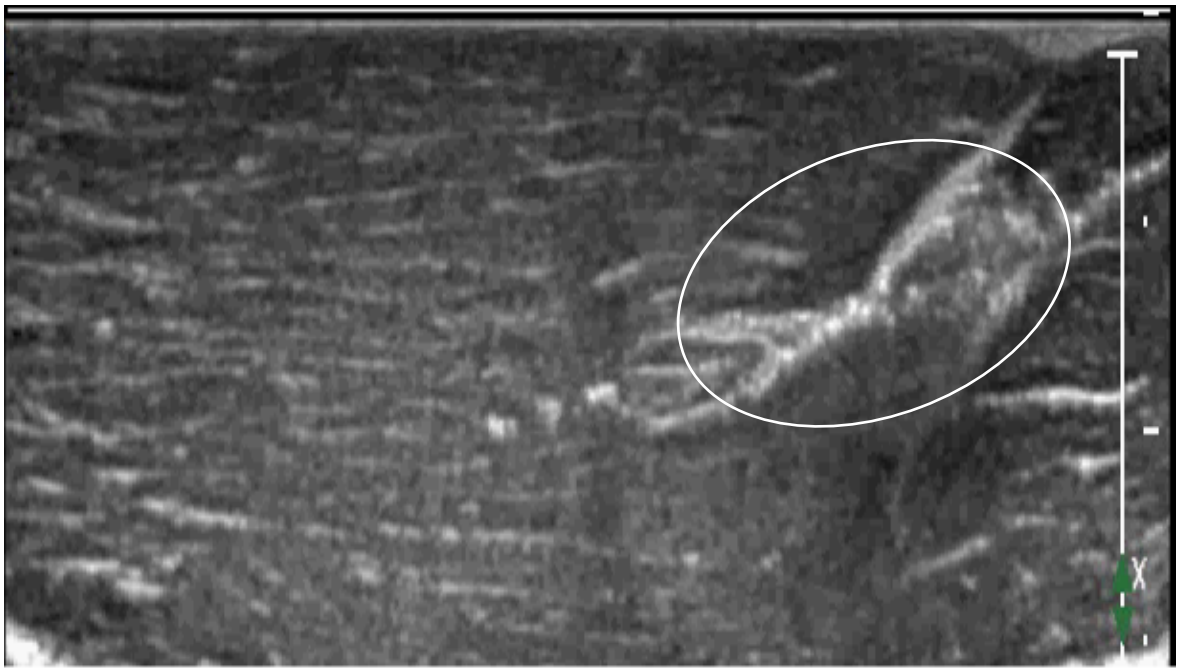

(a) Ultrasound image of the chicken sample model

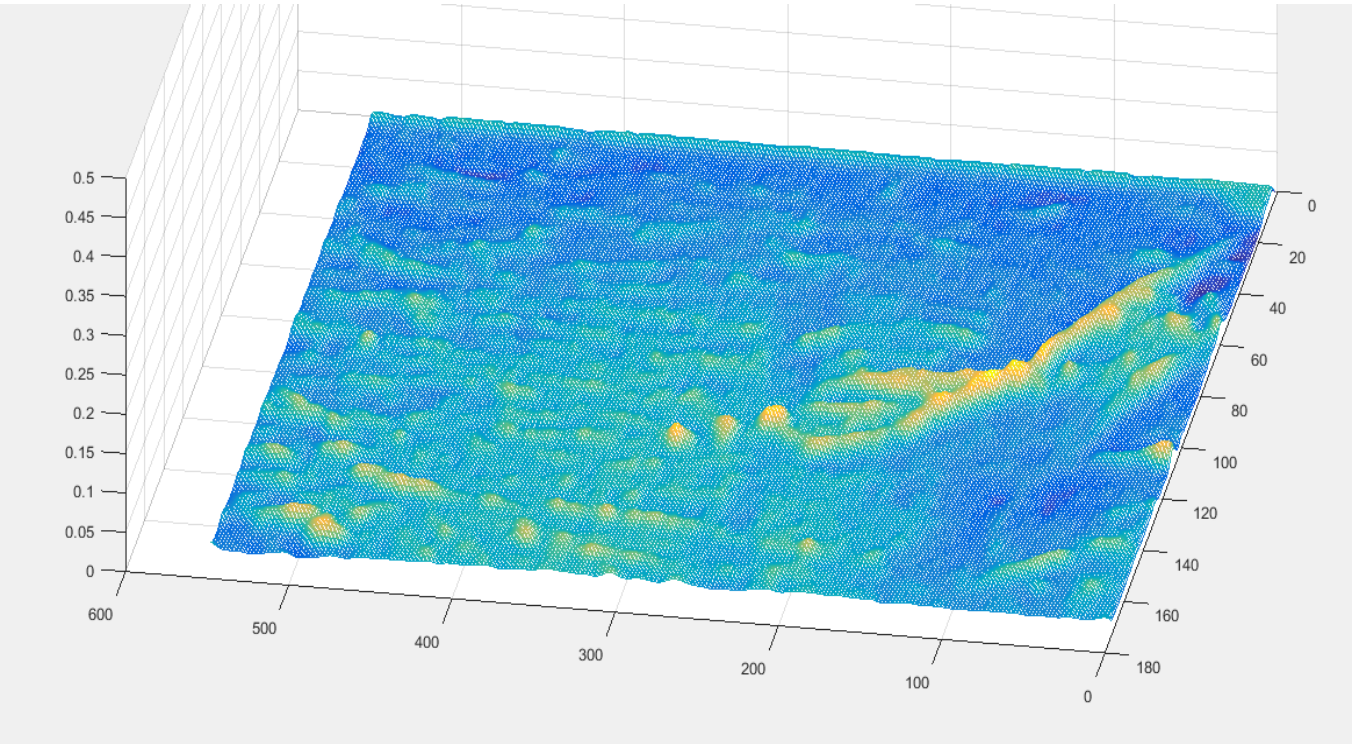

(b) Ensemble average of chicken sample with an abnormality

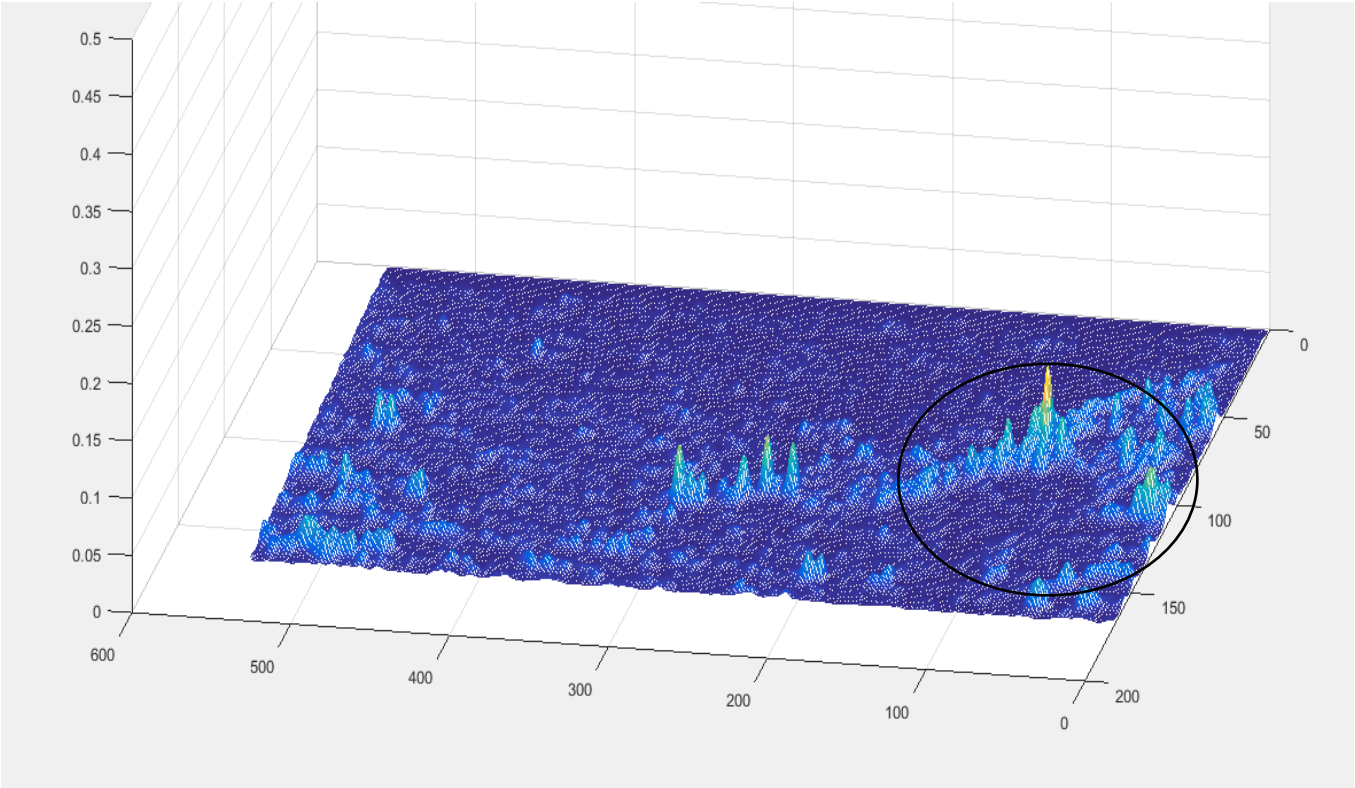

(c) SISA Signature pattern with an abnormality in the chicken tissue

Figure 4.7: Results of ultrasound analysis in Experiment 6 in chicken tissue with an abnormality

From the signature pattern, it can be observed the magnitude on the z-axis, created due to the abnormality, is more than 0.1, whereas, from the previous experiment, in the case of no abnormality present in the tissue magnitude on z-axis didn't exceed 0.05.

In short, *SISA* technique was able to detect the abnormality in chicken tissue model, with different *SISA* scale in the signature pattern compared with pig tissue. In Figure 4.7 (b), the shape and volume of the abnormality can be roughly speculated. The signature pattern in Figure 4.7 (c), becomes very clear about the presence of the abnormality, encircled, in the tissue sample. In the region of interest, the abnormality was detected on the graph through *SISA* processed image.

The abnormality was detected in rough texture of the sample, but no specific conclusion could be drawn in terms of the threshold value, which would create a difference in better detection of normal and abnormal activity.

4.5 Concluding Remarks

Ultrasound medical imaging is very well known for analysis of different tissues and organs in human body. It is also a recommended imaging technique for initial phases in diagnosis of any major problem, and possess no known long-term side effects and hardly cause any trouble to the patients. It allows to explore the insides of human body non-invasively, which itself creates a major difference, in the individual's life such as liver scans, kidney injuries, uterus exams. Whereas, other medical imaging such as CT scan, MRE are equally important with their specialty lying in areas where ultrasound limits. Although, more experimentation is required varying with different type of abnormality with different type of sample. But our preliminary results were very encouraging.

Ultrasound analysis was another step forward for *SISA* image processing. After two sets of experimentation with two animal tissue samples, *SISA* technique showed promising results with better detection algorithm. In experiment 1 and 3 with pig tissues, it was observed that the *SISA* signature pattern is uniform, showing no sign of abnormality, in Figure 4.2 (c) and 4.4 (c), in the given region of interest. But when the abnormality was introduced in the same region of interest for each sample, the *SISA* signature pattern was changed, due to the perturbations caused by abnormality, as shown in Figure 4.3 (c) and 4.5 (c). Although in experiment 5 and 6, due to low thickness in the chicken tissue and different tissue texture as compared with pig tissues, the *SISA* signature pattern was different. From the Figure 4.6 (c) in case of no abnormality, the *SISA* threshold value set for pig tissue was 0.05 but in chicken tissue threshold value was set for 0.1, which implies that different tissue types have different *SISA* signature pattern with different set threshold value, which contribute to different perception in abnormal and normal behavior.

In an overview, after these experiments the use of ultrasound medical imaging with *SISA* processing is solidified for further experimentation and fusion with other medical imaging techniques for a better early detection and localization algorithm for abnormalities in active biological systems.

Chapter 5

CONCLUSIONS

5.1 Summary

The *SISA* approach described in this thesis is an innovative non-invasive approach for the detection and localization of the abnormal activity at an early stage in an active biological system. In this work, we have developed a basic *SISA* approach for processing medical images. This *SISA* approach was preliminarily tested on a liquid vibrating system with and without abnormalities, which was then extended for locating the abnormalities in animal tissues, such as pig and chicken's tissues. Different stages (grades) of the abnormality in the active system, creates different types of *SISA* signature pattern. An abnormality in an early stage, such as a minor damaged tissue, will induce low non-linear impedance (or finite impedance), which creates a small perturbation. However, an abnormality in critical stages, such as completely damaged tissue, will induce a high non-linear impedance, which creates a high wave perturbation, and this high perturbation will be detected by the *SISA* signature pattern.

In this *SISA* approach, image sensors (camera for the liquid vibrating system and ultrasound probe for biological tissues) were fixed on the ROI, and about 200 images for individual experiments were taken at different time intervals. An abnormality creates an anomaly in the active system, which induces non-linear impedance and creates perturbations hindering the smooth flow of processed activities, such as blood flow and electrical signals in the system. In the experiment with the liquid vibrating system, when the abnormality interacts with pseudo-random excitation, it produces extra perturbations, which was observed in the *SISA* signature

pattern. In the preliminary experiment it was found that a threshold value of *SISA* signature pattern could be defined for normal and abnormal cases. The abnormalities like solid obstacle as infinite impedance and perforated obstacle as finite impedance, the *SISA* processing was capable of locating and distinguishing the difference in each abnormality. Similarly, in further experiments with *SISA* on ultrasound analysis in animal tissues, the abnormality was detected in pig and chicken tissues, which showed promising results with *SISA* approach in biological active systems. *SISA* approach is developed to locate and analyze the abnormalities that usually go undetected in other non-invasive medical imaging, they can be examined using signature pattern.

In the final remarks, Space-Invariant Signature Algorithm in preliminary phases displayed very favourable results. This brief study shows that *SISA* is capable of merging with other medical imaging techniques and provides the potential of detecting and localizing abnormalities in early stages with a notable impact on human and animal lives.

5.2 Limitations

Our research was conducted on two set of experiments: preliminary analysis using a liquid vibrating system and ultrasound analysis, using images from these experiments and process using *SISA* algorithm to determine any presence of abnormality. Our methodology was confirmed with both of these experiments but some limitations were observed. Firstly, in our research, early stage abnormality detection is discussed but the details regarding the progression and necessary measurements in order to deem an abnormality as early stage were not discussed. The abnormalities in the experiment were an analogy and simulated the early stage abnormal behavior. Understanding the progression of the abnormality in live models, or conducting more experiments with different types of possible abnormalities can overcome this limitation.

Secondly, the liquid vibrating system experiment was limited to the capability of digital camera in terms of resolution; the camera was capable to capture, perfectly, the pseudo-random wave pattern of a 100 Hz bandwidth signal, which was determined through numerous trial and error experiments. A higher resolution and better digital camera can capture enhanced quality images for improved detection in liquid vibrating system.

5.3 Directions for Future Research

In this thesis, a theoretical study with some experiments has been carried out. In order to further enhance the knowledge with the applications of ultrasound imaging more experiments with different abnormal behaviors needs to be implemented. Other medical imaging techniques such as Elastography, CT scan and MRI can be merged with the *SISA* approach, which will further improve and take this work to another level and will allow us to better understand the behaviour of abnormalities in early stages using this research. SISA approach will also need to account for different variables and factors arising as different imaging techniques use different concepts and display the image in their own way. Early detection is a challenge for many areas and detection in incipient stages simplifies the critical stage problems. For future research and applications, *SISA* approach has the potential and could be a breakthrough in early detection and diagnosis in medical imaging.

APPENDIX A

VARIOUS MEDICAL IMAGING TECHNIQUES

Detection of the abnormality or disease at an early stage is necessary to take sufficient precautionary measures. The old technique for detection is palpation, a process in which the doctor uses his hands to examine the body and to feel the difference in mechanical properties of the tissues, which are suspected. The palpation still remained a best diagnostic tool for physicians. Even today the different sophisticated medical techniques cannot depict the properties that are assessed by palpation. Keeping these facts in mind, palpation is an expertise, which comes after a long practice and is mastered by handful of practitioners. Furthermore, this technique is applicable only to the superficial organs and limited to the sensitivity of the practitioner. Knowing these limitations, it is necessary to have a special detection technique, which provides motivation for early stage localization of abnormalities without solely relying on human hands [41].

Human body is a dynamic complex system. During imaging and acquiring data in humans regarding the detection of disease, it results in massive amount of information to process and creates a challenge to acquire processed and simplified data. Presenting the information as images is the one of the effective ways of representation of the data. Non-invasive imaging of the human body reveal characteristics of the normal and abnormal objects such as transmissivity, opacity, emissivity, reflectivity, conductivity and magnetizability, some of them are discussed below. Thus, medical imaging techniques are prominent to analyze the images for the detection of abnormalities. Some of the major medical imaging techniques is as follows:

A.1 Ultrasonography

Ultrasonography, commonly known as ultrasound is a diagnostic non-invasive imaging technique based on sound waves inaudible to humans (>20KHz). It is used to examine the different body parts such as tissues, internal organs, and blood vessels. Ultrasound images are created by sending sound waves using a probe, the sound echoes through the tissue and reflects back to the probe from different pathways. This wave property is measured by use of pulse-echo method of ultrasound. The velocity of the sound wave travelling inside is proportional to tissue stiffness. As there is significant difference in elasticity of abnormal tissues from normal tissues, the abnormality can be identified.

Another technique that uses ultrasonic waves is, ultrasound Elasticity Imaging (Elastography), it is used to find abnormalities such as cirrhosis, fibrosis. Fibrosis is a condition in which there is a formation of excess fibrous connective tissue in a reparative process due to an injury, and cirrhosis is a condition in which the liver does not function properly due to long-term damage. Assessment of the severity of fibrosis and cirrhosis will often dictate treatment options as well as provide an overall prognosis for patients with chronic liver disease, using non-invasive approaches such as ultrasound elasticity imaging. Invasive method such as liver biopsy, for the detection of fibrosis can be painful, expensive and a risk procedure with complications, but ultrasound elasticity imaging provides a better alternative to this challenge. It measures elastic properties of tissue, which is proportional to velocity of shear wave produced by incidence of ultrasonic waves on the tissue.

Another type of ultrasound is Doppler ultrasound, which is enhanced by using Doppler Effect. It is also a faster, less expensive, non-invasive way in order to determine the blood flow

in the artery, with details such as speed and the direction, which is very useful in cardiovascular studies. An example of Color Doppler in Figure A.1, which is capable of detecting the abnormality and able to represents them in different colors.

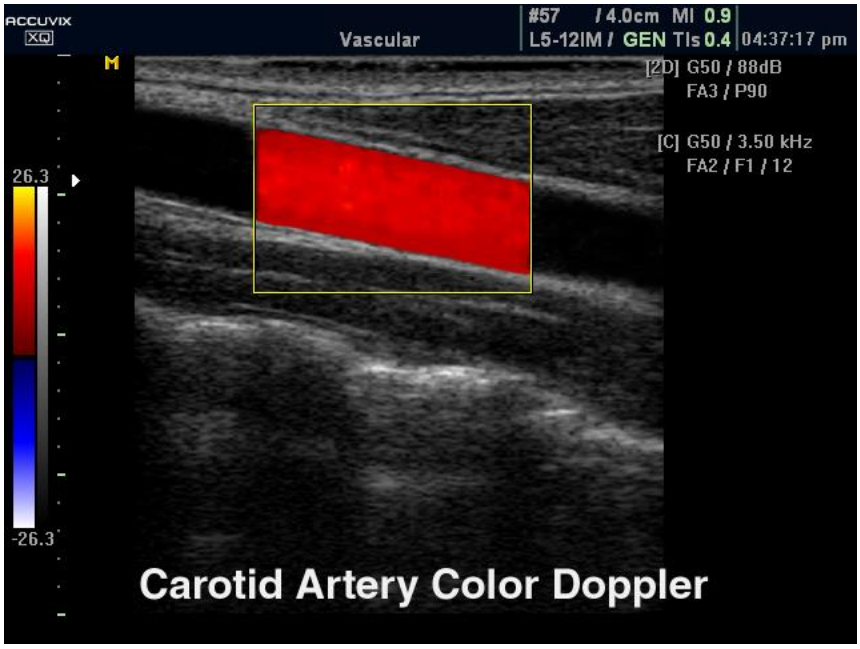

Figure A-1: Carotid Artery Color Doppler (Source: medison.ru)

A.2 Magnetic Resonance Imaging (MRI)

MRI is non-invasive medical imaging techniques that measure the mechanical properties of tissue. Many atoms in their nuclei have a property called “spin”, which is related to the magnetic dipole moment. Human body mainly consists of water that has hydrogen and oxygen atoms. These hydrogen atoms has nuclear spin in different directions, in presence of a strong magnetic field, the nuclear spin aligns and generates an energy difference between spins with or

against the magnetic field. The MRI machine provides the magnetic field through a superconducting solenoid of a specific radio frequency for H-atoms [42].

When the pulse is applied, the unmatched protons of H-atoms absorb the energy and align themselves with the direction of magnetic field. The RF pulse forces them to spin at particular frequency, which is known as Larmor frequency. Larmor frequency is calculated based on particular tissue being imaged and strength of the magnetic field. The frequency of radiation from abnormal tissue is different from normal tissue [41]. MRI takes up to 20 to 90 minutes and requires expensive machinery, which makes it more time consuming and less affordable. During the scan in progress the patient has to be very still in order to achieve better images, which is very hard to do inside the machine that makes a lot of noise for long time [43]. Due to its monetary value, MRI is usually made available for the patients with more urgent problems and prioritizing over less severe problems.

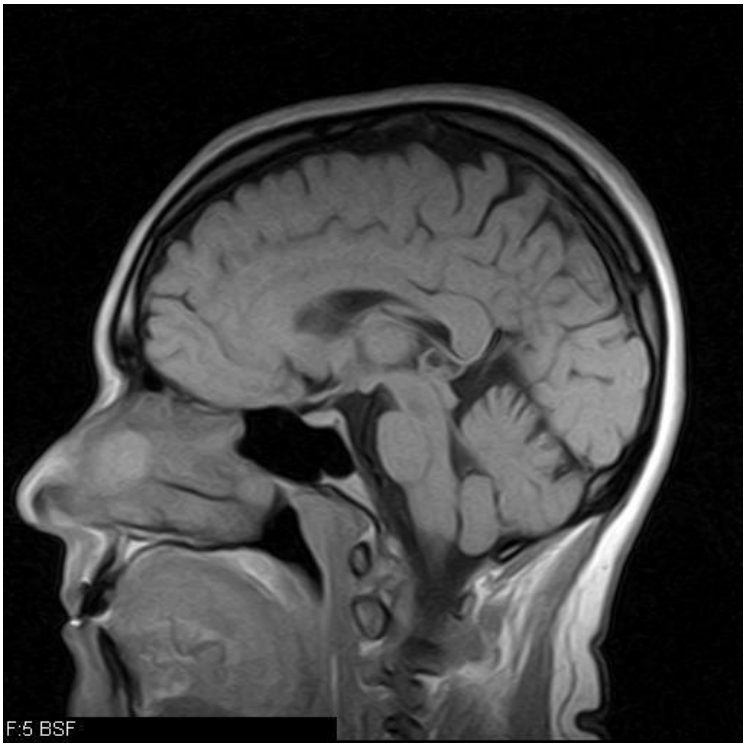

Figure A-2: MRI Scan of the human brain (Source: http://london-imaging.co.uk/)

A.3 CT (Computed Tomography) scan

CT scan uses the traditional idea of X-rays, being able to move through the human body produces multiple images and capable of generating three-dimensional images. Conventional X-rays is a projection of X-rays on a screen, as X-rays travel in straight lines and are absorbed by the bones but not the soft tissues, which allows us to analyze the bone structure in the body. CT images of internal organs, bones, soft tissue and blood vessels provide greater detail than conventional X-rays.

CT scan models the 3D image of the human body by indenting and capturing from different angles. It forms the total 3D image using horizontal "slices", which are obtained by a scanner in one rotation [44].

CT scan is helpful in cancer treatment in many ways [43] [45]:

1) To detect the abnormal growth.
2) To diagnose the presence of the tumor.
3) To provide information regarding the stage of cancer.
4) To detect the recurrence of the tumor.

Besides its advantages, CT scan has some disadvantages too, like even very small amount of ionizing radiation can cause disruption at sub-microscopic level in exposed cells due to long exposure from X-rays, which rips DNA molecule in the cells, causing it more likely to develop a tumor. Although, it depends on many factors that this effect can actually turn into a malignant tumor and it's quite rare during the whole lifetime of a human being, and depending upon the healing ability of the cells. But the malignant transformation of cells at low dose is extremely

unlikely. As long as the benefits outweigh the harmful effects of it, it is recommended to go for the diagnosis [46].

Figure A-3: CT- Scan of human brain.(Source: http://www.conciergeradiologist.com/ct-scan-images.html)

A.4 Vibration Analysis

Hip replacement is a surgical procedure in which the hip joint is replaced by a prosthetic implant. This surgery can be performed as a total replacement or a hemi replacement. The early diagnosis of aseptic loosening of a total hip replacement by plain medical methods like radiography, scintigraphy has been shown to be unreliable. Late loosening with an unstable prosthesis can be reliably detected by a vibration technique called, Vibration Analysis [46].

Vibration Analysis uses a sine-wave generator and a shaker to introduce a sinusoidal force to the implanted prosthesis. The magnitude and frequency of this force were measured using a very sensitive accelerometer placed on the shaker. The vibration signal was transmitted along the bone and detected near the greater trochanter using a second accelerometer. The frequency of the input force was varied along the bandwidth of 100 to 1200 Hz [46].

Distortion of the sinusoidal force occurs when it is passed on a loosened prosthetic system. Spectral analysis of a pure sine wave yields a single peak at the frequency of the sine wave, but spectral analysis of a distorted wave produces multiple additional peaks known as harmonics. The technique is sensitive enough to detect late loosening but not early loosening with minimal or no mechanical instability. [46]

A.5 Angiogram

Angiography (Angiogram) is one of the invasive medical imaging techniques used to visualize inside of blood vessels and organs of the body, which is generally done by injecting a radio-opaque contrast agent into the blood vessel and imaging using X-ray. An angiogram works similar to an X-ray. Normally, blood vessels cannot be seen on an X-ray, but adding a contrast agent into the blood stream makes the blood vessels visible.

Contrast agent contains iodine; a substance that X-rays cannot pass through. To deliver the contrast agent, a catheter is inserted into the large femoral artery in the upper leg. Angiograms are very good at detecting problems with the blood vessels such as an arterial stenosis, tumor, and clots. An angiogram is not without risk as it is an invasive test. There is a

very small risk of the loosening a piece of plaque lining the artery wall. This loose piece of plaque may travel up the artery into the brain and could block blood flow causing a stroke.

APPENDIX B

PHASE -INVARIANT SIGNATURE ALGORITHM: A REVIEW

It was in 1968 when the Theta-Invariant Signature Algorithm (TISA), was developed for processing the high frequency vibrations from rotating machines for early detection, diagnosis and localization of faults such as fault in the bearing or rotating shaft [1, 47, 48]. In early seventies, this TISA approach was extended to *PISA* (Phase- Invariant Signature Algorithm) for processing the high frequency electro-cardiac signals (ECG) for the detection and localization of early ischemic heart diseases, and for processing the high frequency phono-cardiac signals (PCG) for the detection of abnormalities in cardiac valves [2, 49].

For the detection of abnormality in high frequency perturbations in electro-cardiac signals, the *PISA* approach was developed, which was much more sensitive for the detection of early ischemic heart diseases [49, 51]. This approach is capable of detecting cardiac disorders at a very early stage well before their perturbations were visually perceptible in the conventional low frequency ECG [49-51]. The *PISA* approach relies on the fact that disorders in the cardiac system perturb cardiac signals [49, 50]. The detection of these perturbations in the cardiac signals helps in the detection of the cardiac disorders [49-51].

B.1 Mathematical Explanation of *PISA* Approach

In a resting cardiac process, cardiac signals are periodic with a period T, which can be represented in the phase domain, from phase 0 to 2π radians or 0^o to 360^o [49, 51]. For the measurement of electro-cardiac signals the subject under test is kept in the resting position, so

that it can maintain a constant heart rate with the stationary conduction properties of the electro-cardio signal [2, 50-51].

A disorder or abnormality in the heart, such as ischemic cardiac problems, introduces a phase-locked high frequency random perturbation in the electro-cardiac activities, and *PISA* signature pattern provides an indication of these early cardiac abnormalities [51]. Now we give a brief mathematical derivation of *PISA* algorithm [49].

The high bandwidth measured electro-cardiac signal is given by [49]:

$$m(\theta) = s(\theta) + p(\theta) + n(\theta) \quad \text{..... (B.1)}$$

where,

$s(\theta)$ = the stationary carrier component in electro-cardiac signal;

$p(\theta)$ =a phase-locked random perturbation component in the electro-cardiac signal caused by a disorder, such as ischemic cardiac problem;

$n(\theta)$ = the measurement noise.

As a first order approximation assume that a simple additive relationship exists, given in Equation (A.1). The challenge with the *PISA* approach is now to detect the presence of the perturbation $p(\theta)$ caused by a cardiac disorder in the measured cardiac signal $m(\theta)$ [49, 51].

$s(\theta)$ is defined as a stationary component, which can be stated as[49, 50]:

$$E[s(\theta)] = s(\theta) \quad \text{..... (B.2)}$$

where, E[.] represents the ensemble average phase locked to the cardiac cycle. The noise, n(θ) and the perturbation, p(θ) are assumed random components with zero mean value i.e.

$$E[n(\theta)] = 0 \quad \ldots\ldots\ldots\ldots\ldots\ldots\ldots\ldots\ldots\ldots\ldots\ldots\ldots\ldots \quad (B.3)$$

$$E[p(\theta)] = 0 \quad \ldots\ldots\ldots\ldots\ldots\ldots\ldots\ldots\ldots\ldots\ldots\ldots\ldots\ldots \quad (B.4)$$

Both signals, the perturbation component p(θ) and the measurement noise n(θ), are random in nature, but since p(θ) is phased-locked to the cardiac cycle and n(θ) is a measurement noise, which is uniformly distributed over the cardiac cycle, they are assumed to be uncorrelated [49, 50]. Hence the random components are uncorrelated with each other, and with the stationary component, i.e. [49, 50]

$$E[p(\theta)\, n(\theta)] = 0 \ldots\ldots\ldots\ldots\ldots\ldots\ldots\ldots\ldots\ldots\ldots\ldots\ldots\ldots \quad (B.5)$$

$$E[p(\theta)\, s(\theta)] = 0 \quad \ldots\ldots\ldots\ldots\ldots\ldots\ldots\ldots\ldots\ldots\ldots\ldots\ldots\ldots \quad (B.6)$$

$$E[n(\theta)\, s(\theta)] = 0 \quad \ldots\ldots\ldots\ldots\ldots\ldots\ldots\ldots\ldots\ldots\ldots\ldots\ldots\ldots \quad (B.7)$$

Therefore the expectation value of the measurement signal, m(θ) is

$$E[m(\theta)] = E[s(\theta) + p(\theta) + n(\theta)] = s(\theta) \quad \ldots\ldots\ldots\ldots\ldots\ldots\ldots\ldots\ldots\ldots \quad (B.8)$$

Rewriting Equation (A.1), yields the deletion of the stationary component from the measurem1ent and just the random components remaining.

$$m(\theta) - E[s(\theta)] = p(\theta) + n(\theta) \quad \ldots\ldots\ldots\ldots\ldots\ldots\ldots\ldots\ldots\ldots\ldots\ldots \quad (B.9)$$

The power in the random component can be found by taking the expectation value of the square of Equation (A.9):

$$E[\{m(\theta)-E[s(\theta)]\}^2] = E[p^2(\theta) + n^2(\theta) + 2\,p(\theta)\,n(\theta)]$$

$$= E[p^2(\theta) + n^2(\theta)] \quad \text{..... (B.10)}$$

From the left hand side of the Equation (A.9) it can be concluded that the variance of the signal is found. In the right hand side of the equation the power of perturbation and noise component present in the phase of the cardiac cycle [49, 50]. It should be noted that the power in the noise component in Equation (A.9) is independent of phase whereas the power in the perturbation component varies with phase, therefore facilitating the detection of the perturbation [49, 50].

Hence, from the first order approximation a signature process, V1, is defined as [49, 50]:

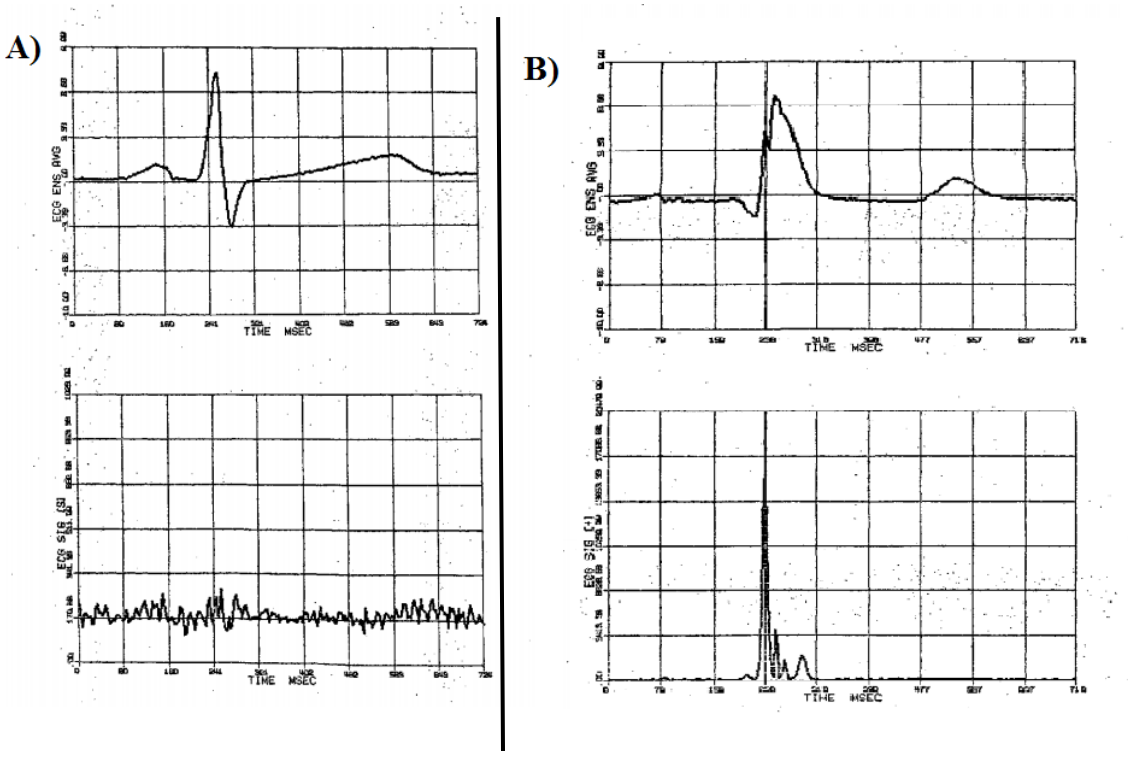

Figure A-4: A) Ensemble average of ECG signal (top) and the PISA signature pattern (below) of a healthy human heart. This amount of variation in the signature is normal and signature is regarded as being flat. B) Ensemble average of ECG signal (top) and the PISA signature pattern (below) of an unhealthy human heart. The large spike in the signature pattern signifies the abnormality.

$$V1\ [m(\theta)]\ | = E[\{m(\theta)-E[s(\theta)]\}^2] \quad \ldots\ldots\ldots\ldots\ldots\ldots\ldots\ldots\ldots\ldots\ (B.11)$$

Figure A-4 shows the results of PISA processing using ECG signal on healthy and unhealthy human heart. This *PISA* approach, as evidenced by wide number of publications [49-52] is found to be very useful for the detection, diagnosis and localization of early ischemic heart disease, as well as heart valve problems.

B.2 Characteristics of *PISA* Approach:

i) No reference is required to compare from the standard measured signal of ECG waveforms or PCG power spectrums is required.

ii) The sensitivity in the *PISA* approach is greater than the conventional ECG and PCG, particularly in case of early disorders. In the early stages of the abnormality, the perturbation component might be below the noise level, and hence, visually undetectable. But the random component of the perturbation would still be detectable through *PISA* signature process.

iii) Aiding cardiologists by extending the information of conventional ECG in detecting the information using *PISA* processing perceived from a different viewpoint of cardiac signal analysis.

REFERENCES

1. Gupta, M. M. & Davall, P. (1977). Theta-Invariant Signature Algorithm (Tisa) For Incipient Failure Detection in Cyclic Machines. 1. Theoretical Development. Transactions of the Canadian Society for Mechanical Engineering, 4(2), 101-106.

2. Prasad, K., and Gupta, M. M. (1978). *PISA*—A new non-invasive method for early detection and quantification of heart disease. *Journal of Molecular and Cellular Cardiology*, *10*, 82.

3. Hanahan, Douglas, and Weinberg, Robert A. (2011). Hallmarks of Cancer: The Next Generation. Cell, 144(5), 646-674.

4. Hanahan, Douglas, and Weinberg, Robert A. (2000). The Hallmarks of Cancer. Cell, 100(1), 57-70.

5. Canadian Cancer Society's Steering Committee on Cancer Statistics. (2012, May). Canadian Cancer Statistics 2012. Toronto, ON: Canadian Cancer Society [Online] Cited: Dec 10, 2015 http://www.cancer.ca/

6. Ebrary, Inc, Public Health Agency of Canada, sponsoring body, and Canadian Cancer Society. Advisory Committee on Cancer Statistics, publisher. (2015). Canadian cancer statistics 2015: Special topic: Predictions of the future burden of cancer in Canada (Canadian cancer statistics; 2015).

7. Fritz, A., Percy, C., Jack, A., Shanmugaratnam, K., Sobin, L., Parkin, D. M., and Whelan, S. (2000). International classification of diseases for oncology (No. Ed. 3). World Health Organization.

8. Emmanuel P. Papadakis (ed) Ultrasonic Instruments and Devices, Academic Press, 1999 ISBN 0-12-531951-7

9. Etzioni, R., Urban, N., Ramsey, S., Mcintosh, M., Schwartz, S., Reid, B. Hartwell, L. (2003). Early detection: The case for early detection. Nature Reviews Cancer, 3(4), 243-252.

10. Canadian Cancer Society (2016) -"Finding Cancer Early". Cited: 20 September 2015. [Online] http://www.cancer.ca/

11. Barretina, J., Caponigro, G., Stransky, N., Venkatesan, K., Margolin, A. A., Kim, S., Garraway, L. A. (2012). The Cancer Cell line encyclopedia enables predictive modelling of anticancer drug sensitivity. Nature, 483(7391), 603-7.

12. Statistics Canada. Canadian Cancer Registry. Available at: http://www23.statcan.gc.ca/ imdb/p2SV.pl?Function=getSurveyimdbandadm=8anddis =2 (accessed on Nov. 19, 2014).

13. Desmetz, C., Mange, A., Maudelonde, T., and Solassol, J. (2011). Autoantibody signatures: progress and perspectives for early cancer detection. Journal of cellular and molecular medicine, 15(10), 2013-2024.

14. Hangiandreou, N. J. (2003). AAPM/RSNA Physics Tutorial for Residents: Topics in US: B-mode US: Basic Concepts and New Technology 1. Radiographics, 23(4), 1019-1033.

15. FDA Radiological Health – "Ultrasound Imaging". [Online] Retrieved on 2015-11-13.http://www.fda.gov/

16. Loeve, M. (1977) "Probability Theory", Graduate Texts in Mathematics, Volume 45, 4th edition, Springer-Verlag, p. 12

17. Rauh-Hain, J. A., Krivak, T. C., del Carmen, M. G., and Olawaiye, A. B. (2011). Ovarian Cancer Screening and Early Detection in the General Population. *Reviews in Obstetrics and Gynecology*, *4*(1), 15–21.

18. Mol, B. W., Boll, D., De Kanter, M., Heintz, A. P. M., Sijmons, E. A., Oei, S. G., ... and Brölmann, H. A. (2001). Distinguishing the benign and malignant adnexal mass: an external validation of prognostic models. Gynecologic oncology, 80(2), 162-167.

19. Zagzebski, J. A. (1996). Essentials of ultrasound physics St Louis. Mo: Mosby.. [Textbook]

20. Karpiouk, A. B., Aglyamov, S. R., Ilinskii, Y. A., Zabolotskaya, E. A., and Emelianov, S. Y. (2009). Assessment of shear modulus of tissue using ultrasound radiation force acting on a spherical acoustic inhomogeneity. Ultrasonics, Ferroelectrics, and Frequency Control, IEEE Transactions on, 56(11), 2380-2387.21. Gullino PM. Tumor pathophysiology: the perfusion model. Antibiot Chemother. 1980;28:35–42.

22. Jain, R. (2001). Delivery of molecular and cellular medicine to solid tumors. Advanced Drug Delivery Reviews, 46(1-3), 149-168.

23. Vaupel, P., Kallinowski, F., and Okunieff, P. (1990). Blood flow, oxygen consumption and tissue oxygenation of human tumors. In Oxygen transport to tissue XII (pp. 895-905). Springer US.

24. Hoyt, K., Sorace, A., and Saini, R. (2012). Volumetric Contrast-Enhanced Ultrasound Imaging to Assess Early Response to Apoptosis-Inducing Anti-Death Receptor 5 Antibody Therapy in a Breast Cancer Animal Model. Journal of Ultrasound in Medicine, 31(11), 1759-1766.

25. Vaupel, P., Kallinowski, F., and Okunieff, P. (1989). Blood flow, oxygen and nutrient supply, and metabolic microenvironment of human tumors: a review. Cancer research, 49(23), 6449-6465.

26. Hoyt, K., Sorace, A., and Saini, R. (2012). Quantitative mapping of tumor vascularity using volumetric contrast-enhanced ultrasound. Investigative Radiology, 47(3), 167-74.

27. Acker, J. C., Dewhirst, M. W., Honore, G. M., Samulski, T. V., Tucker, J. A., and Oleson, J. R. (1990). Blood perfusion measurements in human tumours: evaluation of laser Doppler methods. International Journal of Hyperthermia, 6(2), 287-304.

28. Gillies, R. J., Schomack, P. A., Secomb, T. W., and Raghunand, N. (1999). Causes and effects of heterogeneous perfusion in tumors. Neoplasia, 1(3), 197-207.

29. Molls, M., Vaupel, P., and Brown, J. M. (Eds.). (1998). Blood perfusion and microenvironment of human tumors: implications for clinical radiooncology. Springer Verlag. pp. 41–46.

30. Wilder, J., and Patel, K. (2014). The clinical utility of FibroScan(®) as a noninvasive diagnostic test for liver disease. Medical Devices (Auckland, N.Z.), 7, 107-14.

31. Lignon, Boursier, Delumeau, Michalak-Provost, Lebigot, Oberti, and Aubé. (2015). Screening for significant chronic liver disease by using three simple ultrasound parameters. European Journal of Radiology, European Journal of Radiology.

32. Canadian Academy of Health Sciences. (2010). Making an impact: a preferred framework and indicators to measure returns on investment in health research. [Online] Retrieved from http://www.cahsacss.ca/e/assessments/completedprojects.php

33. Guth, S., Theune, U., Aberle, J., Galach, A., and Bamberger, C. M. (2009). Very high prevalence of thyroid nodules detected by high frequency (13 MHz) ultrasound examination. *European journal of clinical investigation*,*39*(8), 699-706.

34. Kim, E. K., Park, C. S., Chung, W. Y., Oh, K. K., Kim, D. I., Lee, J. T., and Yoo, H. S. (2002). New sonographic criteria for recommending fine-needle aspiration biopsy of nonpalpable solid nodules of the thyroid. American Journal of Roentgenology, 178(3), 687-691.

35. Lacout, A., Chevenet, C., Thariat, J., Figl, A., and Marcy, P. Y. (2013). Qualitative ultrasound elastography assessment of benign thyroid nodules: Patterns and intra-observer acquisition variability. The Indian journal of radiology and imaging, 23(4), 337.

36. Mahoney, M., Sorace, A., Warram, J., Samuel, S., and Hoyt, K. (2014). Volumetric contrast-enhanced ultrasound imaging of renal perfusion. Journal of Ultrasound in Medicine: Official Journal of the American Institute of Ultrasound in Medicine, 33(8), 1427-37.

37. Garner, A. E., Lewington, A. J., and Barth, J. H. (2012). Detection of patients with acute kidney injury by the clinical laboratory using rises in serum creatinine: comparison of proposed definitions and a laboratory delta check. Annals of clinical biochemistry, 49(1), 59-62.

38. Thakar, C. V., Christianson, A., Freyberg, R., Almenoff, P., and Render, M. L. (2009). Incidence and outcomes of acute kidney injury in intensive care units: A Veterans Administration study. Critical care medicine, 37(9), 2552-2558.

39. Obermüller, N., Geiger, H., Weipert, C., and Urbschat, A. (2014). Current developments in early diagnosis of acute kidney injury. International urology and nephrology, 46(1), 1-7.

40. Kalantarinia, K. (2009). Novel imaging techniques in acute kidney injury. Current Drug Targets, 10(12), 1184-1189.

41. William R. Hendee, Author, E. Russell Ritenour, Kenneth R. Hoffmann, and Reviewer. (2003). Medical Imaging Physics, Fourth Edition. Medical Physics, 30, 730.

42. Muthupillai, R., Lomas, D., Rossman, P., Greenleaf, J., Manduca, A., and Ehman, R. (1995). Magnetic Resonance Elastography by Direct Visualization of Propagating Acoustic Strain Waves. Science, 269(5232), 1854-1857.

43. American College of Radiology and Radiological Society of North America "Patient Safety: Radiation Dose in X-Ray and CT Exams". Retrieved July 19, 2013.

44. Harris, Tom. "How CAT Scans Work" 18 April 2002. HowStuffWorks.com. <http://science.howstuffworks.com/cat-scan.htm> Cited: 19 May 2015. Online.

45. Frush, D. P., Donnelly, L. F., and Rosen, N. S. (2003). Computed tomography and radiation risks: what pediatric health care providers should know. Pediatrics, 112(4), 951-957.

46. Li, P., Jones, N., and Gregg, P. (1995). Loosening of total hip arthroplasty. Diagnosis by vibration analysis. The Journal of Bone and Joint Surgery. British Volume, 77(4), 640-4.

47. Douce, J. L., Ng, K. C., & Gupta, M. M. (1966). Dynamics of the parameter-perturbation process. Electrical Engineers, Proceedings of the Institution of, 113(6), 1077-1083.

48. Gupta, M. M. (1967). Dynamics of the Parameter-perturbation Process: With Applications to the Parameter Optimization Process (Doctoral dissertation, University of Warwick).

49. Graham, B. (1976)."Phase invariant signature analysis of cardiac signals." PhD diss., Thesis (Ph. D.)--University of Saskatchewan.

50. Prasad, K., Gupta, M. M., & Graham, B. L. (1978). A Preliminary Study in the Detection of Cardiac Disorders via Phase-Invariant Signature Algorithm of ECG. *Japanese heart journal*, *19*(3), 383-395.

51. Prasad, K., & Gupta, M. M. (1981). *PISA*: A noninvasive method in detection and quantification of acid-induced myocardial infarction in dogs. Clinical cardiology, 4(4), 180-187.

52. Gupta, M. M., & Prasad, K. (1980). Studies of the effects of glucagon on ouabain-induced cardiac disorders using the *PISA* method. Advances in myocardiology, 1, 313.